Supramolecular Chemistry and Molecular Self-Assembly

M2 – Ecole polytechnique - Université Paris-Saclay France

Calyxarenes, dendrimers and other examples

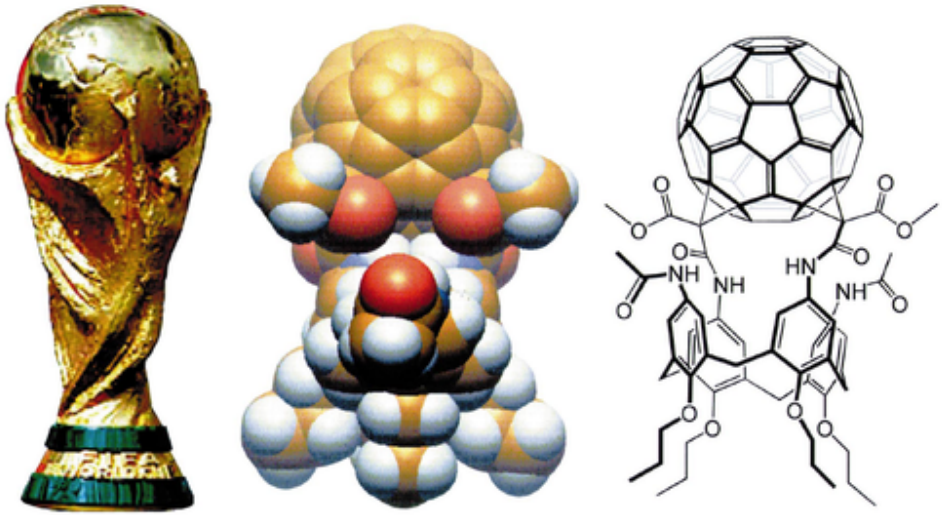

Relazione di forma tra la coppa del mondo di calcio (sinistra) e il coniugato fullerene-calix[4]arene nel modello a palle (centro) e rappresentazione schematica (destra).

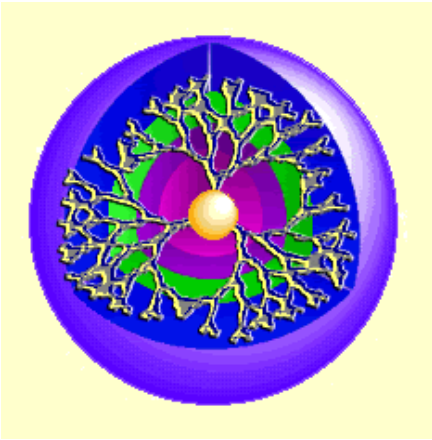

Outline

1. Thermodynamic and kinetic aspects
2. Calyxarenes, dendrimers and other examples
3. Supramolecular chemistry in diagnosis and therapeutic chemistry
4. Supramolecular chemistry in the environment
5. Discussion

Design and Synthesis of Calixarenes: nomenclature

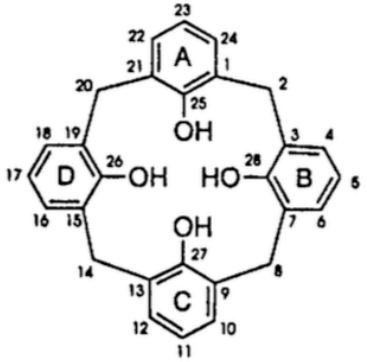

calix[4]arene-25,26,27,28-tetrol

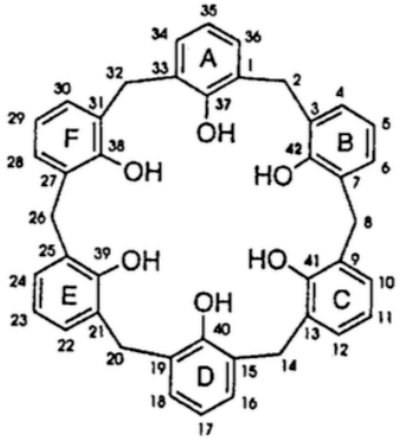

calix[6]arene-36,37,38,39,40,41,42-hexol

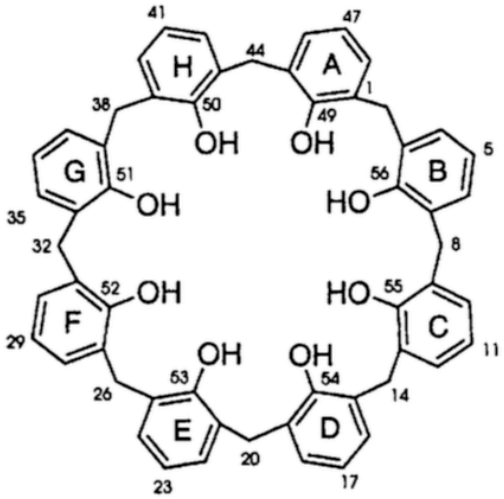

calix[8]arene-49,50,51,52,53,54,55,56-octol

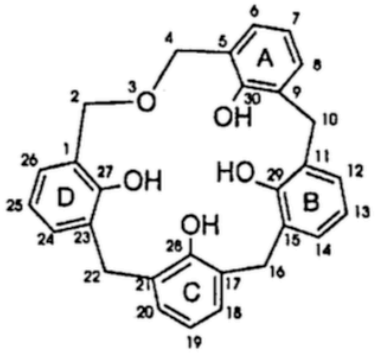

2,3-dihomo-3-oxacalix[4]arene-27,28,29,20-tetrol

Figure 1.5 *Nomenclature of calixarenes*

Design and Synthesis of Calixarenes: conformations

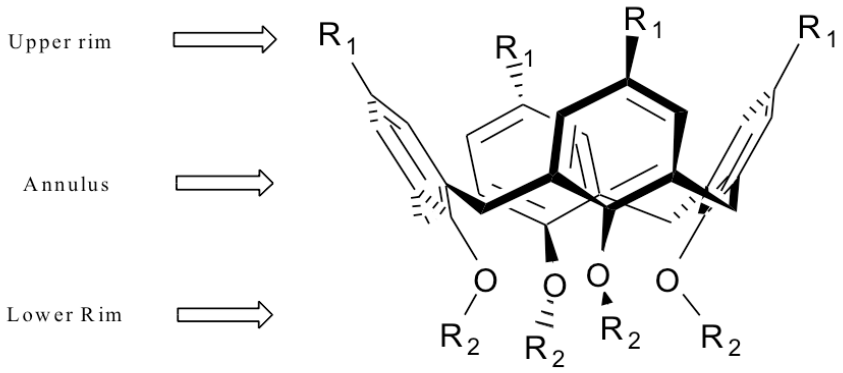

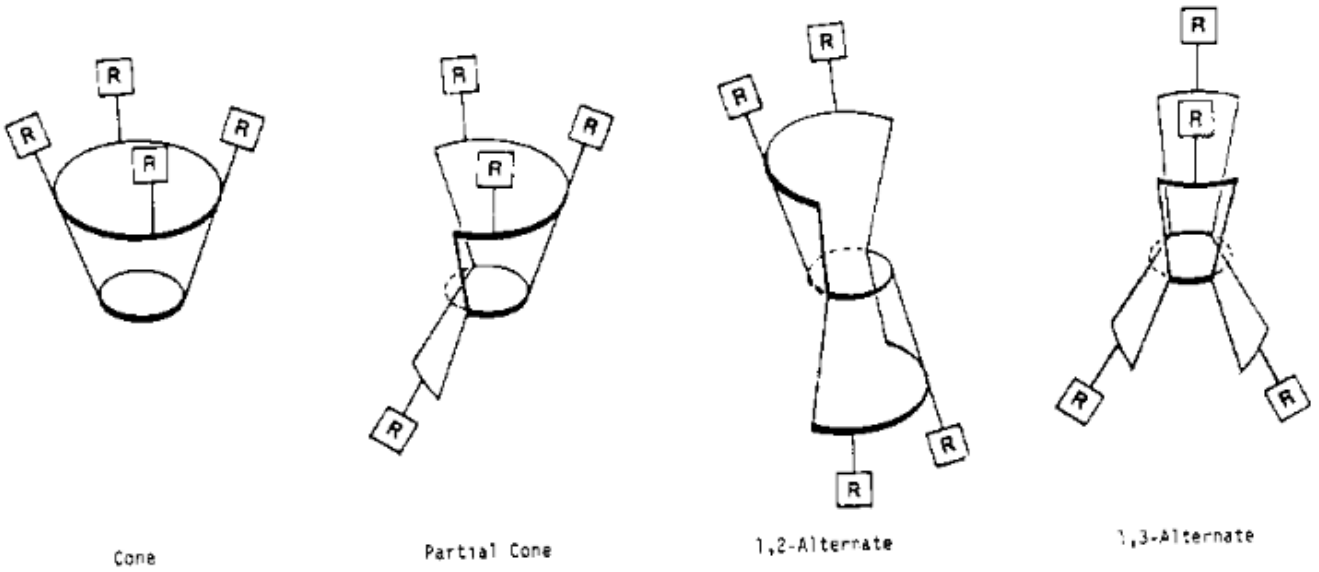

Figure 1. Conformations of the calix[4]arenes.

Gutsche, C. D. et al., *J. Am. Chem. Soc.*, **1985**, *107*, 6052

Design and Synthesis of Calixarenes: conformations

Gutsche, C. D. et al., *J. Am. Chem. Soc.*, **1985**, *107*, 6052

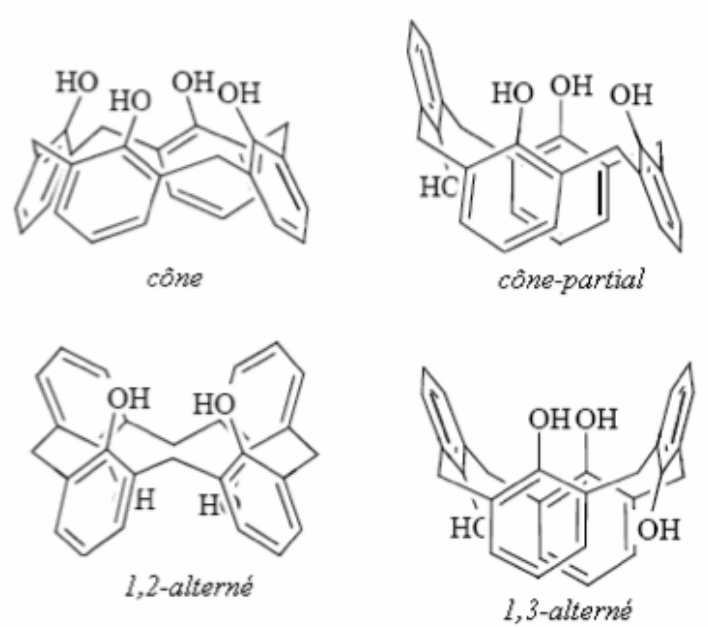

Table I. Coalescence Temperatures, Methylene Shift Positions, and Free Energies of Activation for the Conformational Inversion of the Calix[4]arenes (**1**) at 100 MHz

para substituent	deuterated solvent	T_c, °C	methylene shifts, Hz H(A)	methylene shifts, Hz H(B)	$\Delta G^{\ddagger}$, kcal/mol
tert-butyl	chloroform	52	425	350	15.7
	bromobenzene	43	423	337	15.2
	toluene	39	425	324	14.9
	carbon disulfide	36	427	351	14.9
	benzene	35	423	336	14.8
	pyridine	15	472	360	13.7
hydrogen	chloroform	36	425	352	14.9
	bromobenzene	23	434	333	14.1
	toluene	18	416	314	13.9
	benzene	15	420	327	13.8
	acetonitrile	0	411	346	13.3
	acetone	−5	418	361	13.1
	pyridine	−22	478	345	11.8
phenyl	chloroform	44	443	373	15.3
	bromobenzene	36	433	353	14.9
	acetone	8	435	389	13.8
	pyridine	−2	521	378	12.8
allyl	chloroform	37	420	343	15.0
	acetone	5	413	352	13.5
	acetonitrile	2	409	343	13.3
tert-octyl[a]	chloroform	30	427	350	14.6
	bromobenzene	24	426	344	14.3
	toluene	28	423	325	14.4
	pyridine	−13	467	371	12.4
tert-amyl	chloroform	27	423	350	14.5
	bromobenzene	25	427	338	14.3
	toluene	36	424	322	14.8
isopropyl	chloroform	33	426	350	14.8
	bromobenzene	32	430	334	14.6
	toluene	30	428	322	14.4
benzoyl	chloroform	33	435	370	14.9
hydroxyethyl	chloroform	44	422	343	15.3
	acetone	18	428	307	13.8
dichlorodi-*tert*-butyl	chloroform	38	423, 420	347, 343	15.0
bromo	pyridine	2	492	350	13.0

[a] *tert*-Octyl is the designation used for 2,2,4,4-tetramethylbutyl.

Design and Synthesis of Calixarenes: conformations

Substituents in lower and upper rims

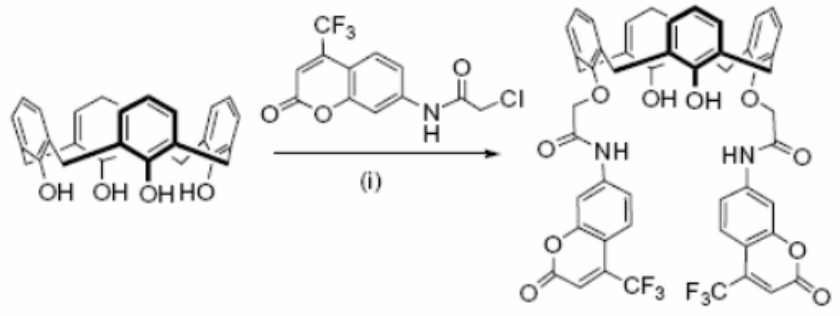

Lee et al., *Tetrahedron Lett.*, **2006**, *47*, 4373 **Cone**

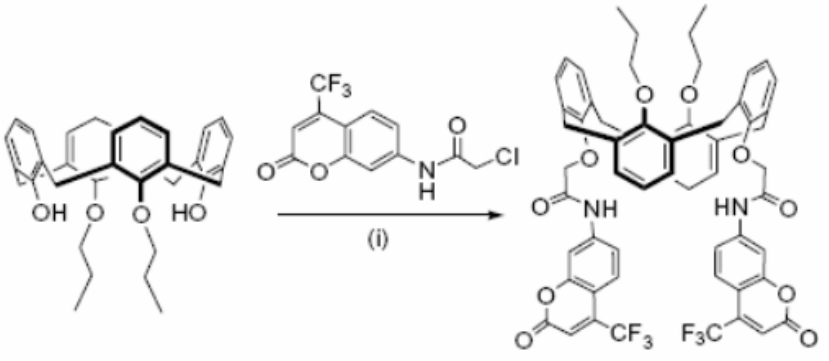

(i) K_2CO_3, NaI, CH_3CN, N_2 **1,3-alternate**

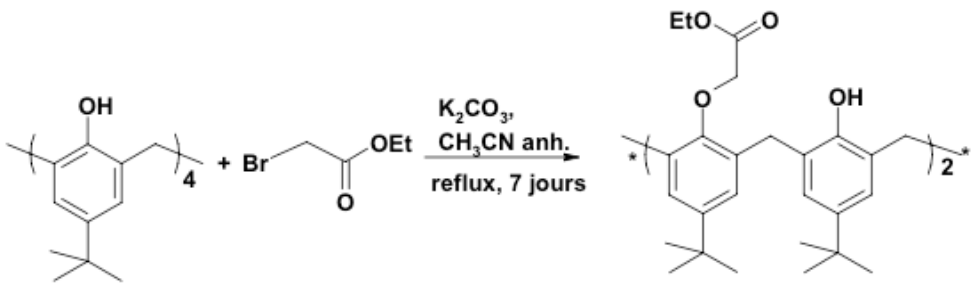

Cone

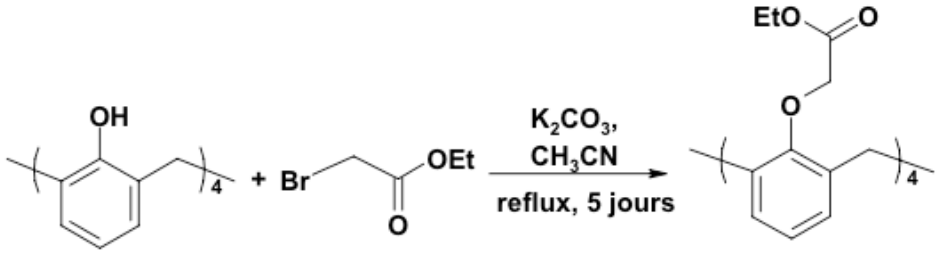

1,3-alternate

Design and Synthesis of Calixarenes: conformations

Reaction conditions

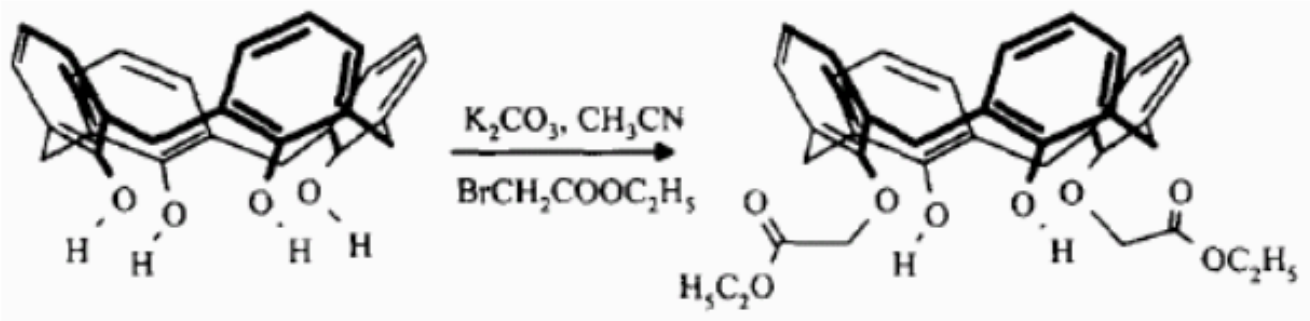

Cone

Arena et al., *Tetrahedron Lett.*, **1997**, *38*, 1999

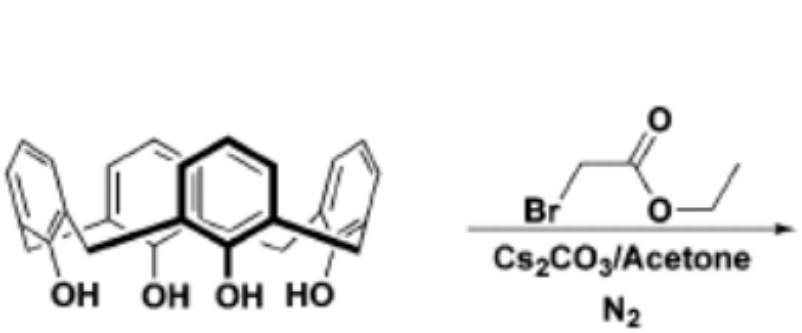

Kim et al., *Inorg. Chem.*, **2005**, *44*, 1846

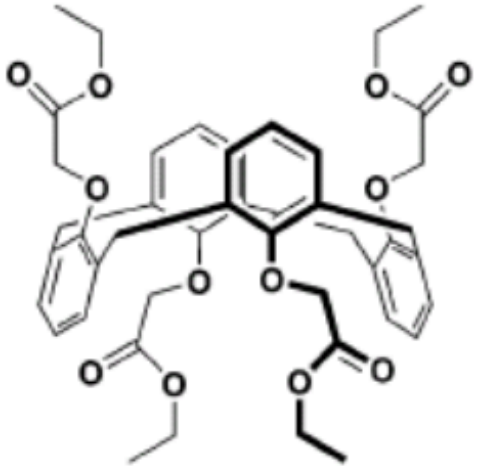

1,3-alternate

Calixarenes: Applications

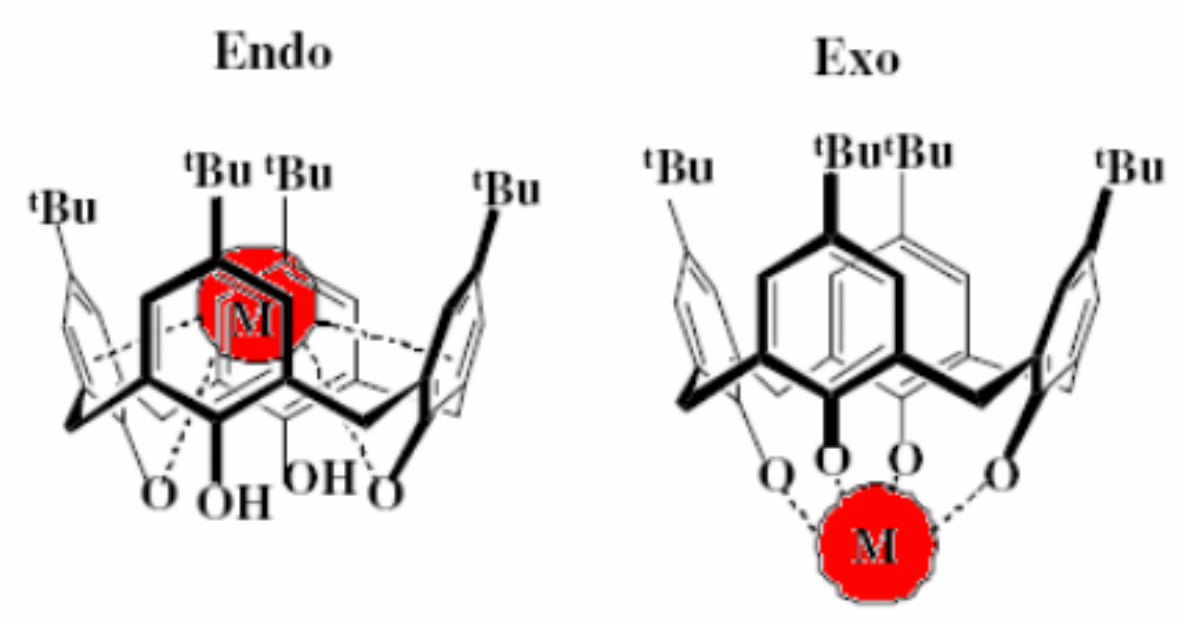

- Biologic applications (therapeutic and vectorization) **See next lecture**
- Environmental applications **(nuclear wastes)**

  See lecture on environmental application

- **Molecular recognition**

Calixarenes: Molecular recognition

Baldini et al., Calixarenes in Molecular Recognition

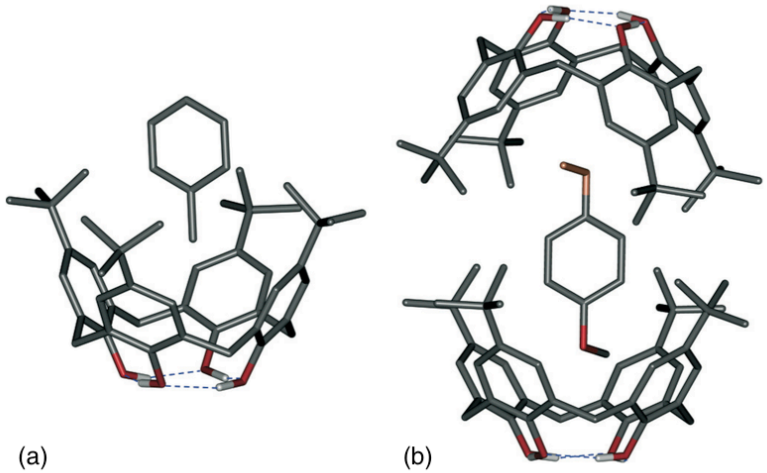

Figure 7 X-ray crystal structure of (a) 1 : 1 complex between **1** and toluene and (b) 2 : 1 complex between **1** and anisole (one of the two statistically equivalent OCH_3 groups is colored in orange).

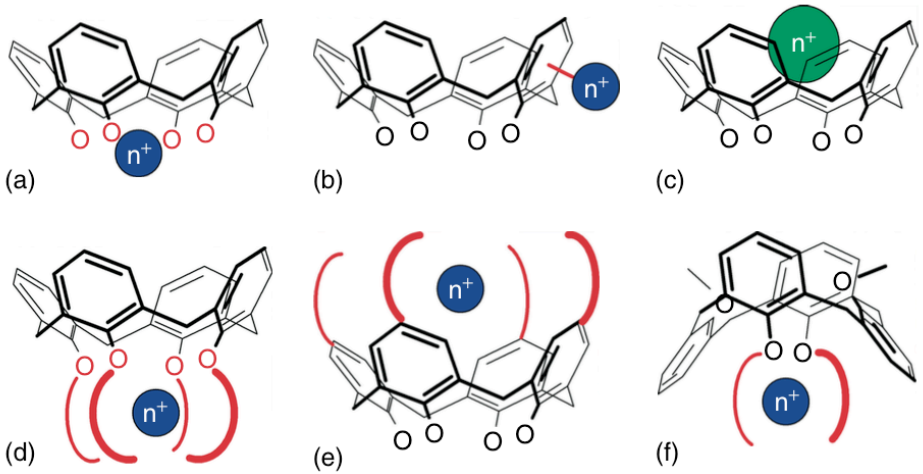

Figure 13 Different ways in which calixarenes interact with cations: (a) metallation at the *lower rim*; (b) *exo*-cavity (π-metallation); (c) *endo*-cavity; (d) at the *lower rim* with participation of additional binding sites; (e) at the *upper rim* by coordinating groups; (f) at the *lower rim* with participation of cation–π interactions. O atoms at the lower rim may be O^-, OH or OR.

Calixarenes: Molecular recognition

Baldini et al., Calixarenes in Molecular Recognition

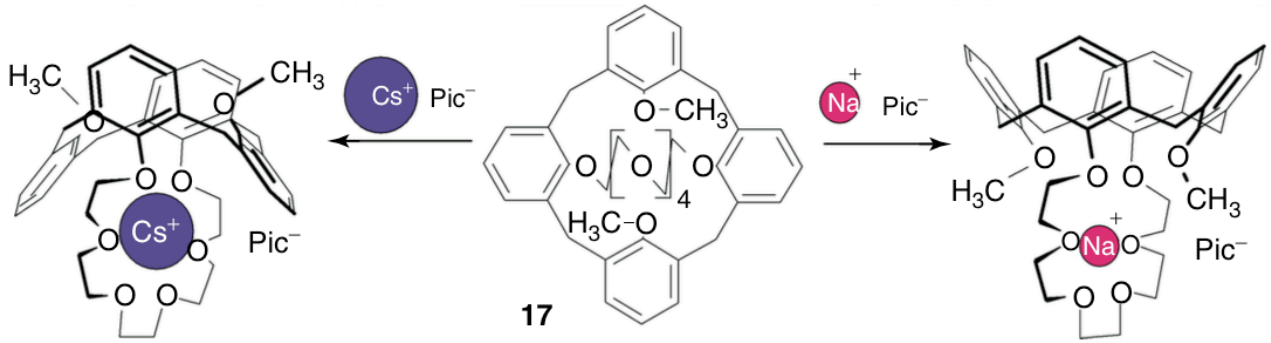

Figure 14 Conformational interconversion upon caesium or sodium binding by calix-crown-6 (**17**).

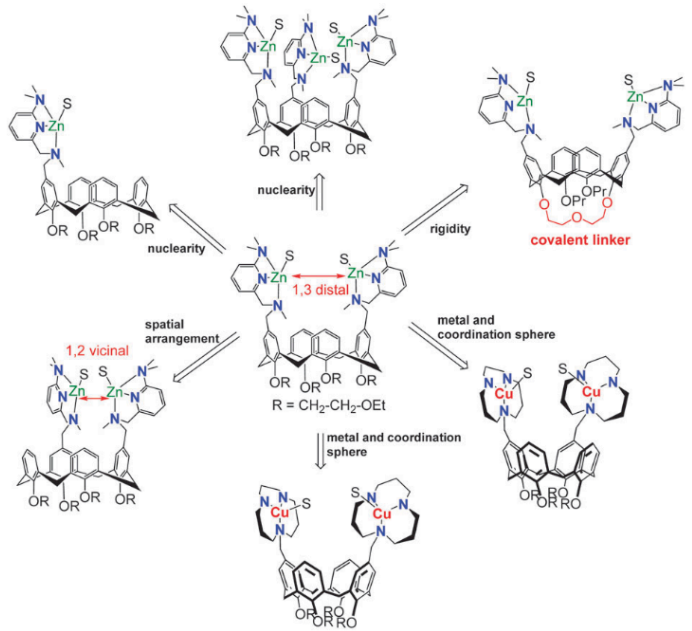

Fig. 1 Zinc(II) and copper(II) complexes built on a calix[4]arene platform.

Reinaud et al., *Chem. Soc. Rev.*, **2015**, *44*, 467

Calixarenes: Molecular recognition, an example

Scheme 1. General Strategy for the Design of the Calix[6]arene-Based Systems Acting as Biomimetic Molecular Funnels

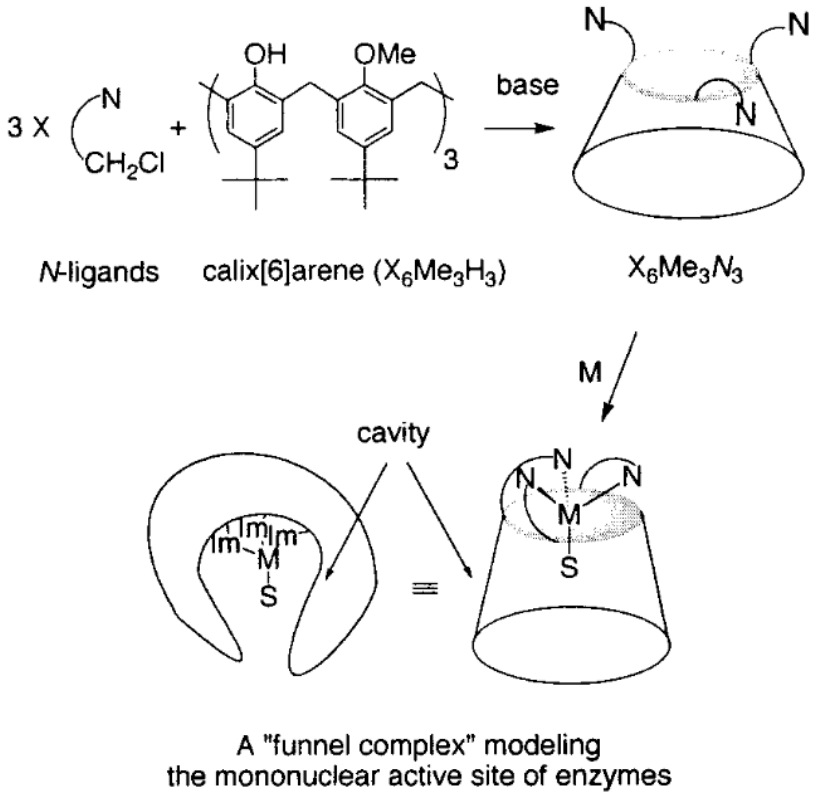

A "funnel complex" modeling the mononuclear active site of enzymes

Reinaud et al., *J. Am. Chem. Soc.*, **2000**, *122*, 6183

Scheme 3. Ligand Exchange in the Cavity of the Zinc "Funnel Complexes"[a]

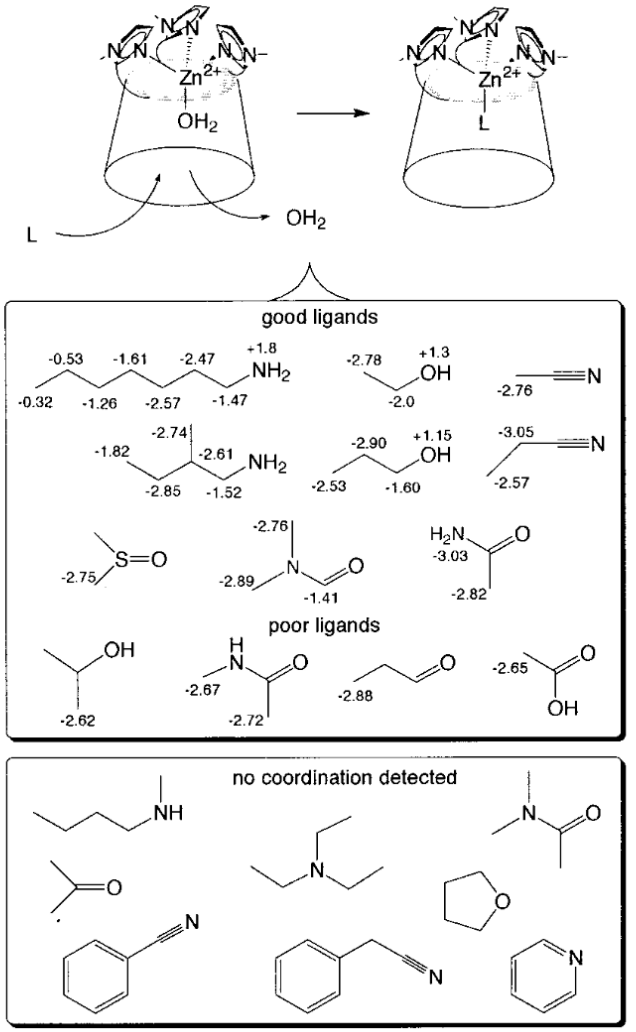

[a] The $\Delta\delta$ shifts observed by ^{1}H NMR spectroscopy for the guest ligand are indicated next to the corresponding atoms ($\Delta\delta = \delta_{\text{coordinated L}} - \delta_{\text{free L}}$. δ is the chemical shift; in some cases, $\delta_{\text{coordinated L}}$ could not be determined because of peaks overlapping).

Calixarenes: Molecular recognition, an example

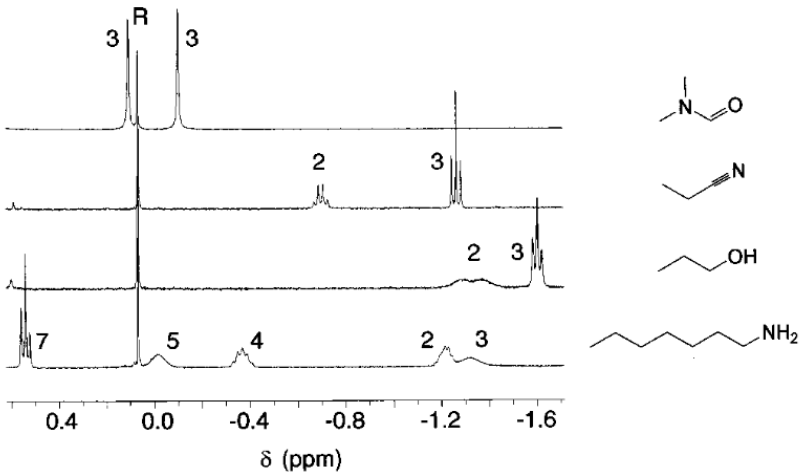

Figure 2. High-field region of the ^{1}H NMR spectra of [Zn(X_6Me_3-Imme$_3$)(L)](ClO$_4$)$_2$ in $CDCl_3$ at 297 K (400 MHz). From top to bottom, L = DMF, EtCN, PrOH, *n*-HeptNH$_2$. The relative protons' positions to the coordinating heteroatom (Y = N, O) are indicated with numbers. The reference peak is labeled "R".

Table 1. Equilibrium Constants K_{L/H_2O} for the Ligand Exchange (L vs H_2O) at the Zn^{2+} Center, in the Cavity of the Calixarene

substrate L	K_{L/H_2O}
heptylamine	>100
dimethyl sulfoxide	21 (5)
acetamide	28 (7)
dimethylformamide	4.0 (8)
N-methylacetamide	0.15 (9)
ethanol	20 (6)
propan-1-ol	1.3 (5)
propan-2-ol	0.04 (1)
acetonitrile	1.7 (5)
propionitrile	0.6 (3)

Reinaud et al., *J. Am. Chem. Soc.*, **2000**, *122*, 6183

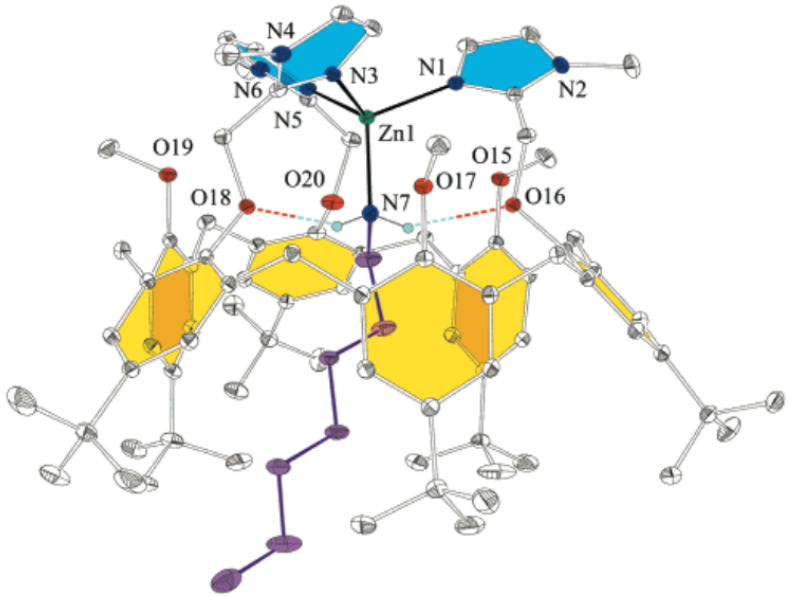

(i) The tris(imidazole) donor set that wraps the metal center, thereby capping the cone of the calix[6]arene,

(ii) The neutral environment that exacerbates the acidic character of Zn^{2+},

(iii) The hydrophobic calixarene cavity, which controls the exchange processes at the metal center, and

(iv) The presence of hydrogen- bond acceptors that can stabilize an acidic guest.

Dendrimers: History

Introduced in 1985 by D. A. Tomalia and G. R. Newkome

Dendrimers are globular, size monodisperse macromolecules in which all bonds emerge radially from a central focal point or core with a regular branching pattern and with repeat units that each contribute a branch point.

The first inspiration for synthesizing such molecular level treelike structures evolved from a lifetime hobby enjoyed by Donald Tomalia

Concept of repetitive Grow with branching was reported in 1978 by Buhleier

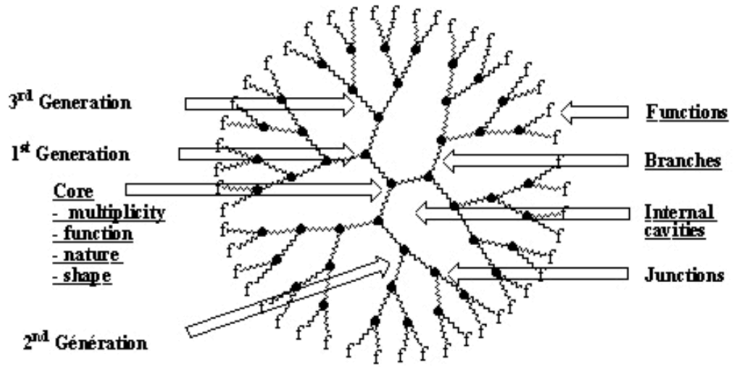

4th Generation Dendrimer

Dendrimers: History

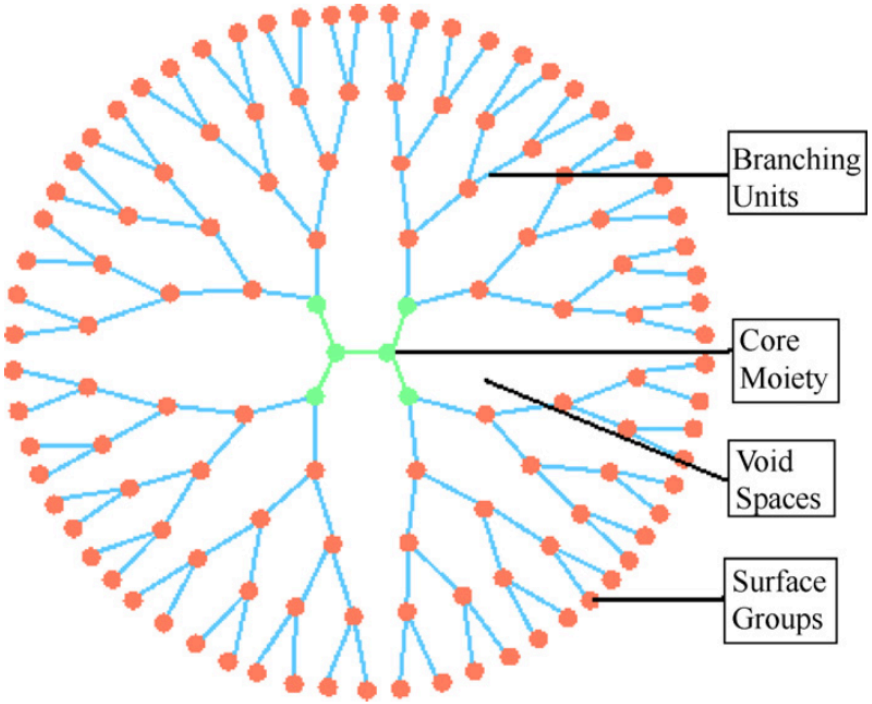

Fig. 1. Schematic representation of generation 4 dendrimer.

Najwade et al., *European Journal of Pharmaceutical Sciences,* **2009**, *38*, 185

(polyamidoamine)

Table 1
Physical characteristics of PAMAM dendrimers.

Generation	Number of surface groups	Molecular weight[a]	Diameter (nm)[b]
0	4	517	1.5
1	8	1,430	2.2
2	16	3,256	2.9
3	32	6,909	3.6
4	64	14,215	4.5
5	128	28,826	5.4
6	256	58,048	6.7
7	512	116,493	8.1
8	1024	233,383	9.7
9	2048	467,162	11.4
10	4096	934,720	13.5

[a] Molecular weight is based on defect-free, ideal-structure, amine terminated dendrimers.
[b] Molecular dimensions determined by size-exclusion chromatography.

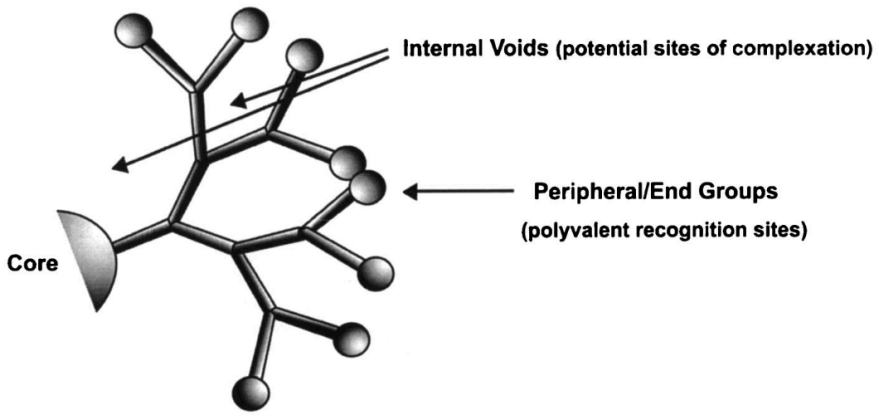

Fig. 2. Schematic showing the three main parts of a dendrimer, the core, end-groups, and sub-units linking the two

Dendrimers: Synthesis

In divergent synthesis, the dendrimer molecule grows outwards from the core. The first generation of the molecule is created through the reaction between the core molecule and molecules containing one reactive and two dormant groups. More branches are formed as reactions occur, eventually resulting in the formation of generations.

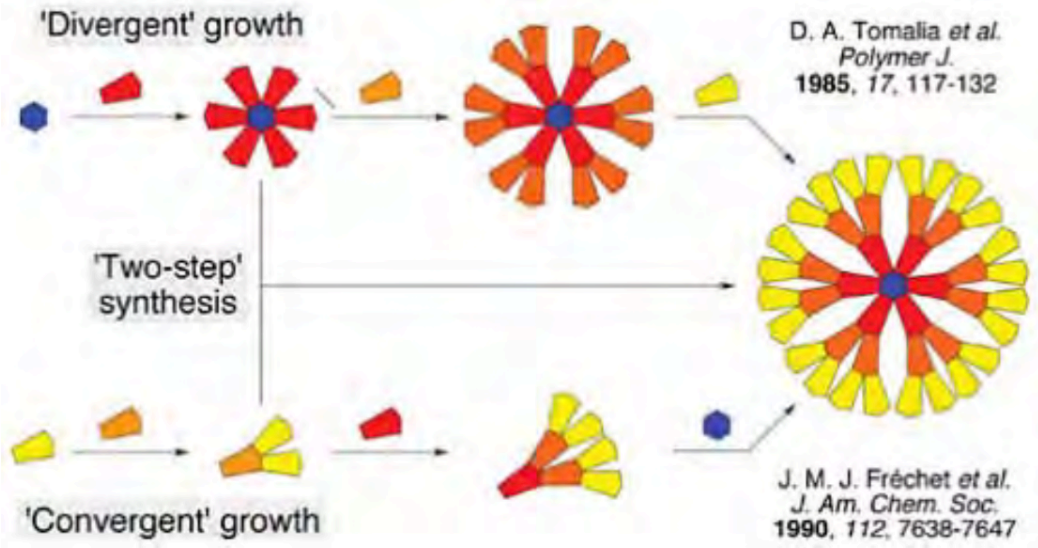

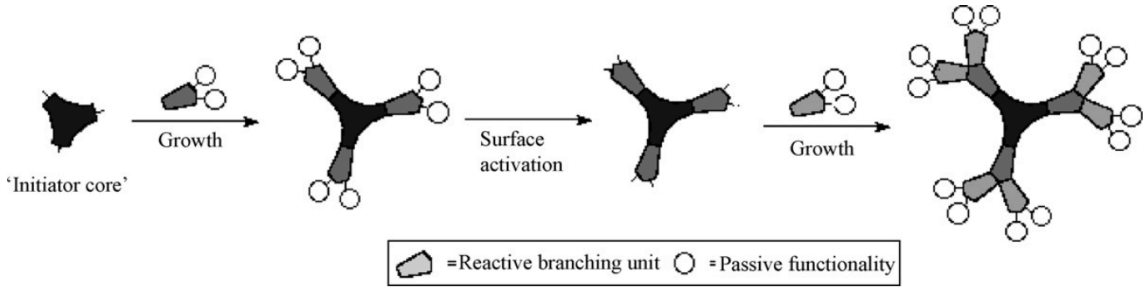

Fig. 2. Divergent growth method.

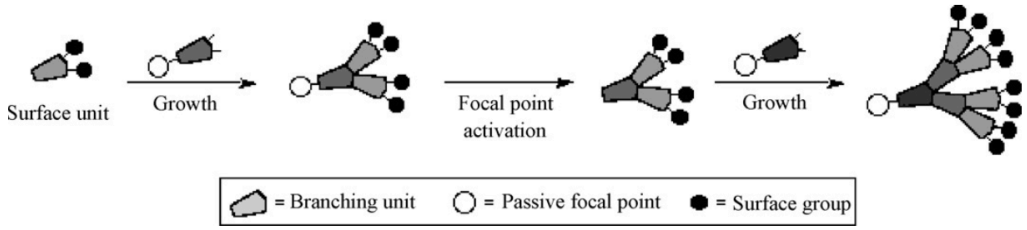

Fig. 3. Convergent growth method.

The divergent method of synthesis is useful when creating large amounts of dendrimers. However, there are cons, which include side and incomplete reactions at end groups. To prevent these occurrences, a large excess of reagents is needed, which make purification of the final product much more difficult.

Dendrimers: Synthesis

The creation of convergent synthesis was a response to defects surrounding the divergent synthesis method. This method is the complete opposite of the divergent method, because it grows molecules from the outside inwards. Branches grow larger as they progress towards the core, and eventually attach themselves to the center. Convergent synthesis addresses many problems of divergent synthesis. For example, it is easy to purify the product, and there are minimal structural defects. However, it is not perfect, as high generation dendrimers cannot be formed.

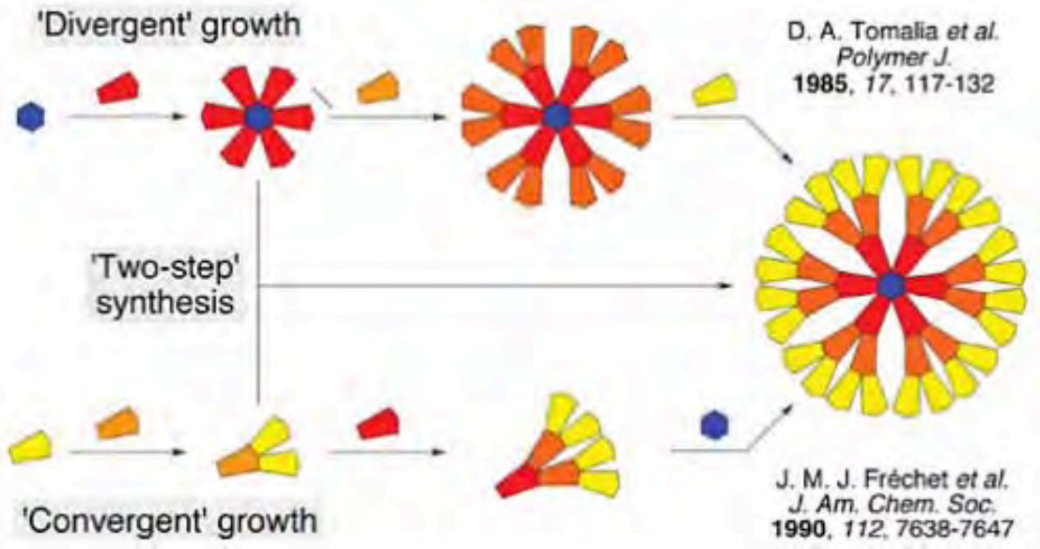

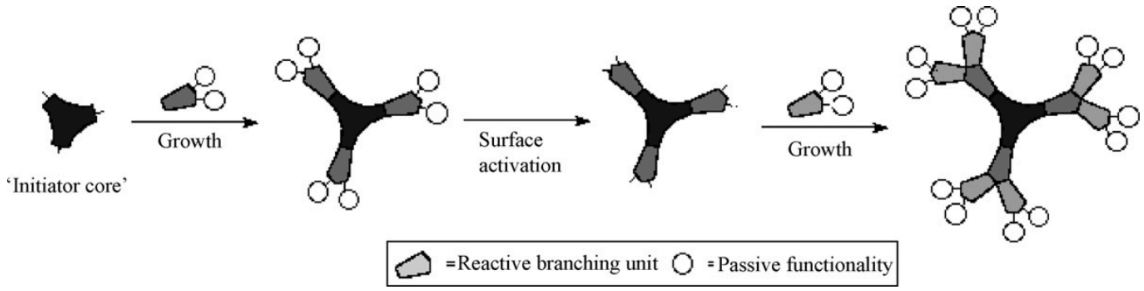

Fig. 2. Divergent growth method.

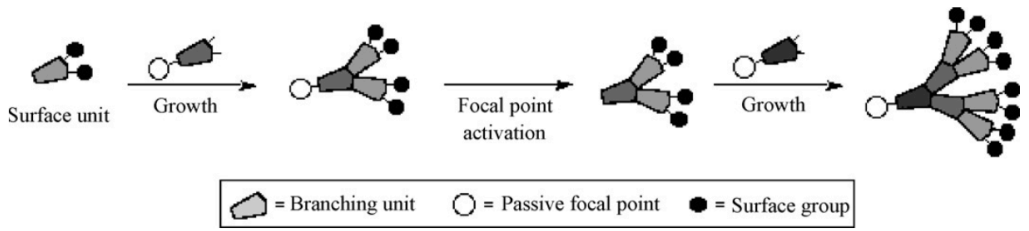

Fig. 3. Convergent growth method.

Dendrimers: Covalent dendrimers

Unimolecular Micelle

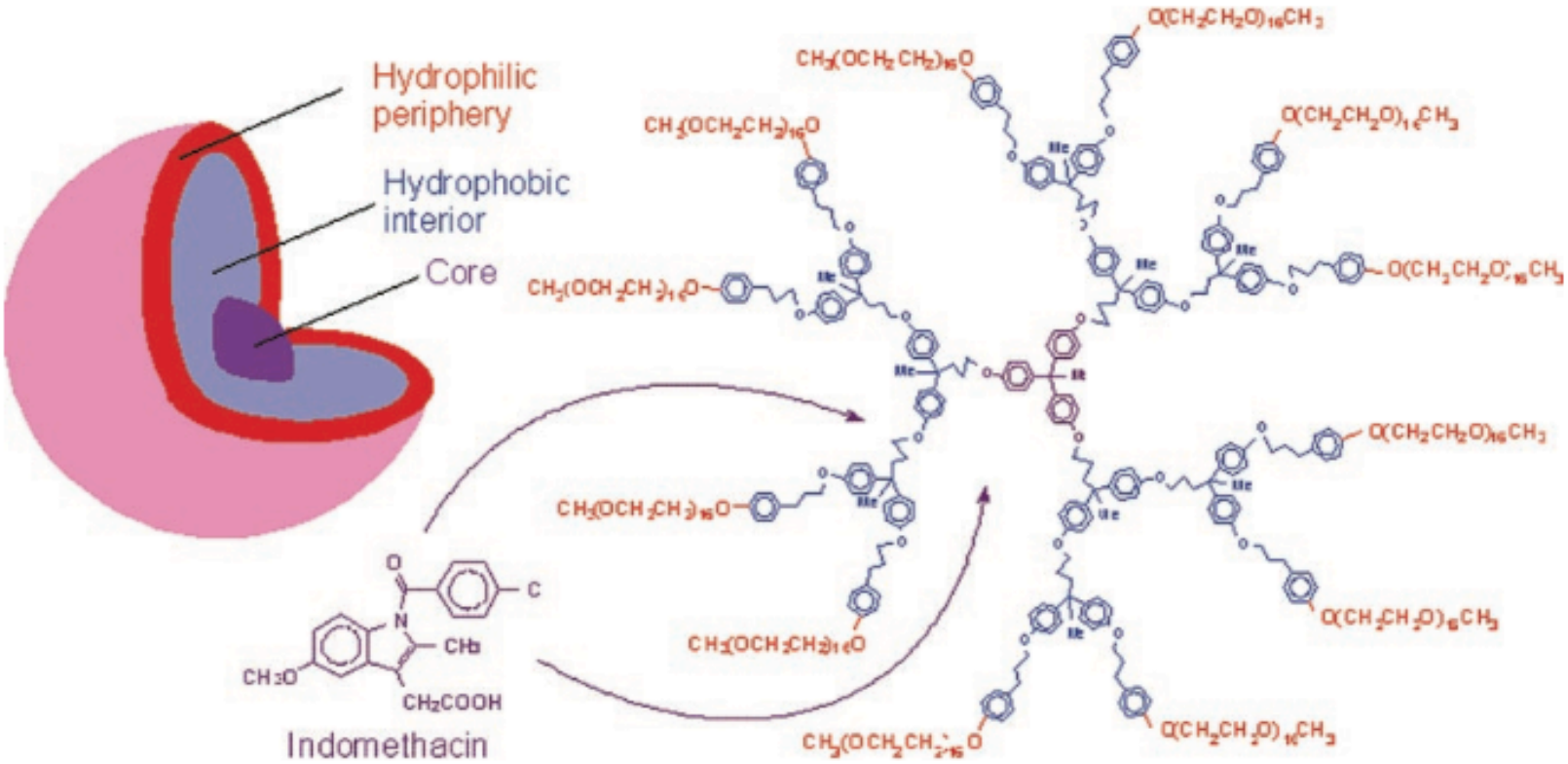

Fig. 4. Dendritic "unimolecular micelle" used for the slow release of indomethacin.

Fréchet, J. M. J. J. Controlled Release, **2000**, *65*, 121

Dendrimers: Self Assembly

Hydrogen bond mediated Self-Assembly

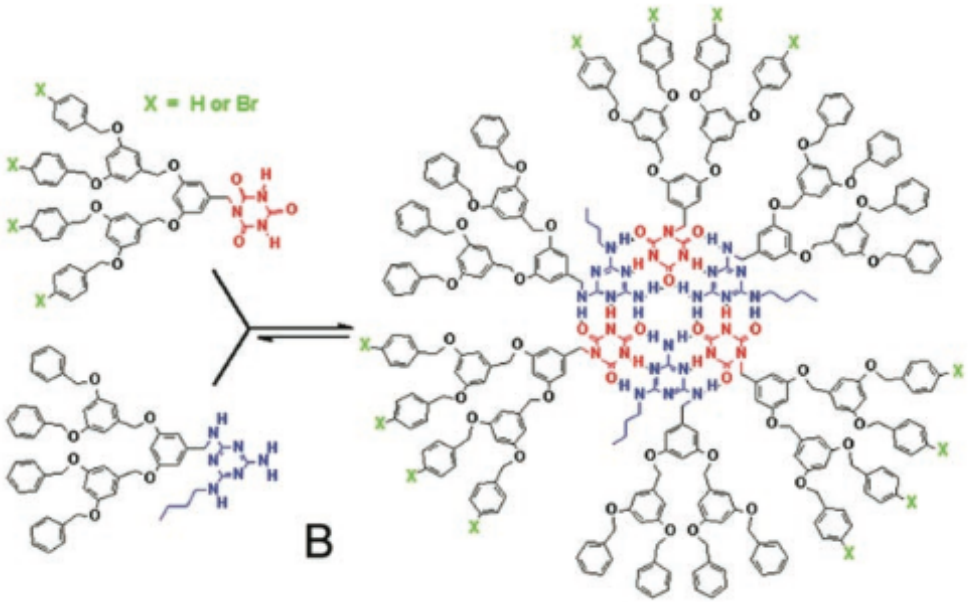

Fréchet

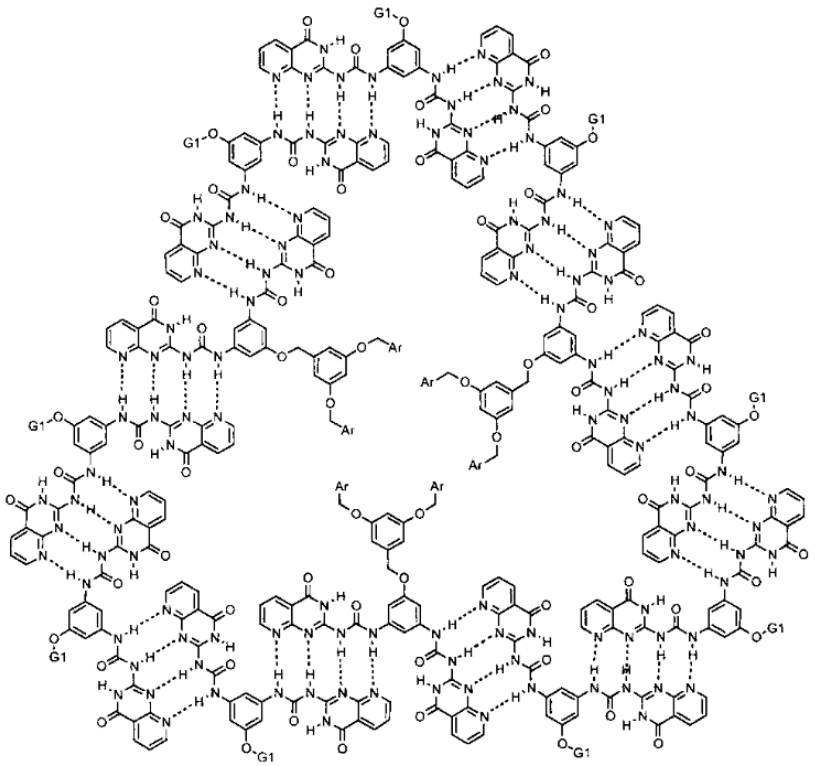

17 : Ar = 3,5-di(t-Bu)Ph

Fig. 10. Structure of dodecameric assembly **17**.

Zimmerman, PNAS, 2001

Dendrimers: Self Assembly

Metal Complexation Mediated Self-Assembly

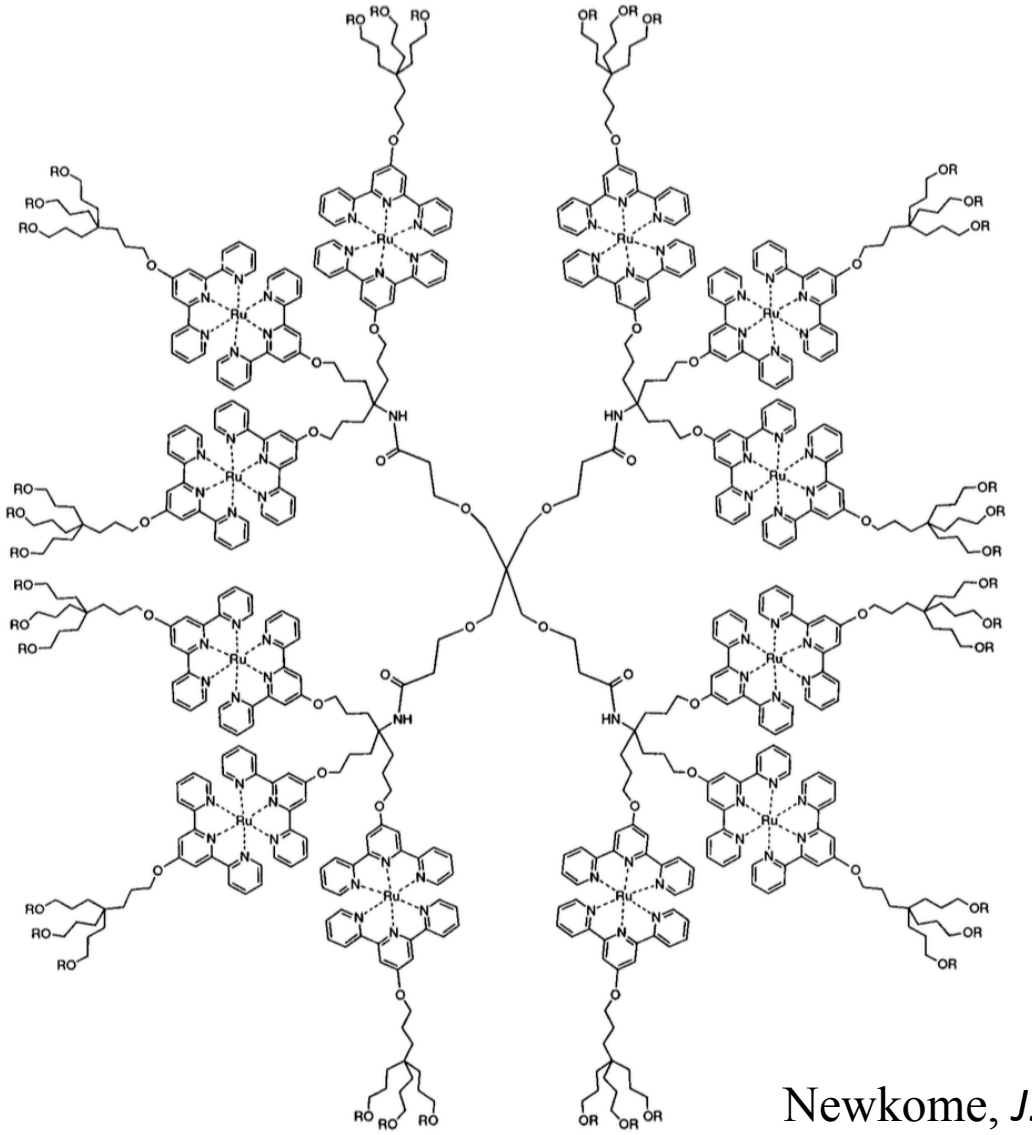

Newkome, *J. Chem. Soc., Chem. Commun.* **1993**, 925

Dendrimers: Self Assembly

Metal Complexation Mediated Self-Assembly

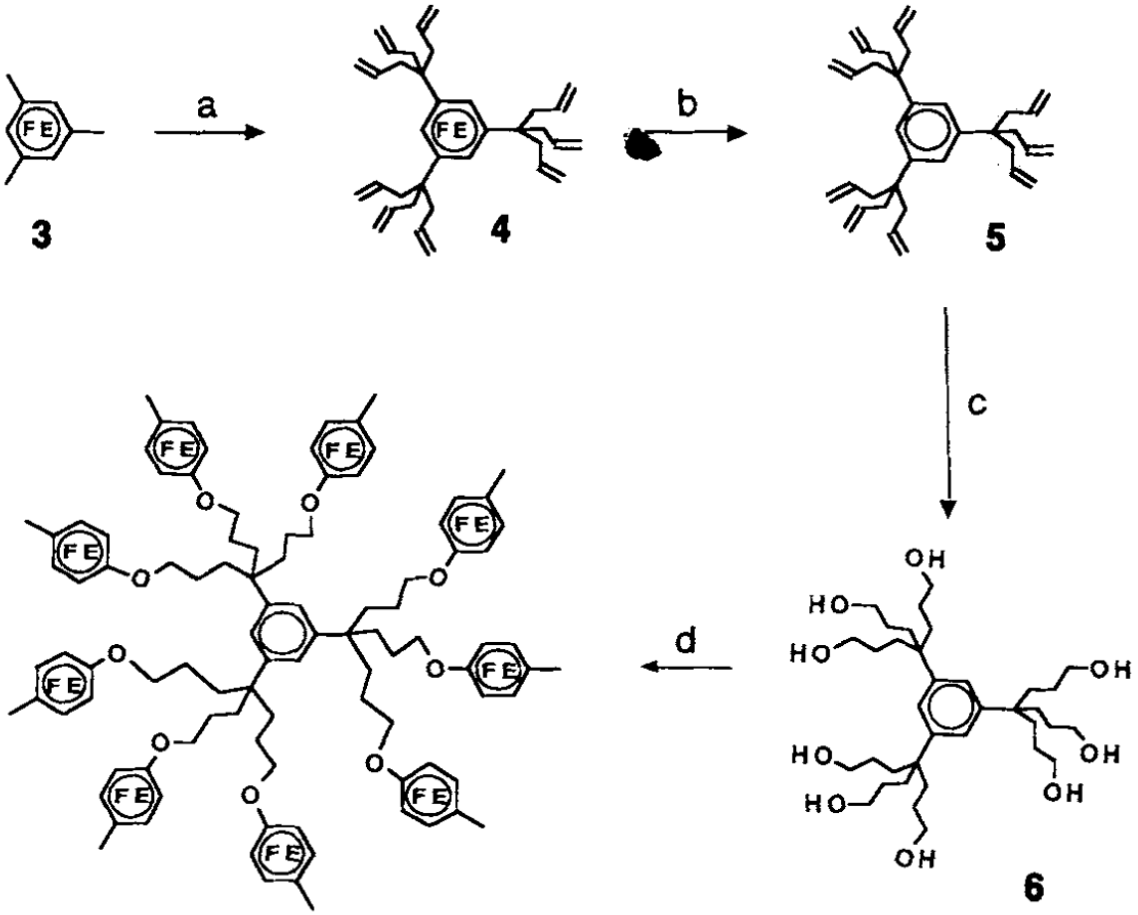

Scheme 1. Synthesis of the nonacation **7**. a) CH_2CHCH_2Br, KOH, DME, 20 °C, 9 days; b) MeCN, PPh_3 (1 equiv), visible light, 7 h, 25 °C; c) Disiamylborane $(Me_2CHCHMe)_2BH$, THF, 20 °C, 1 day, 30% H_2O_2, 3 M NaOH, 50 °C, 1 h; d) $[Fe(Cp)(\eta^6\text{-}p\text{-}MeC_6H_4F)]PF_6$, K_2CO_3, $(Bu_4)NBr$, THF/DMSO (80:20), 20 °C, 3 days.

Astruc, *Angew. Chem., Int. Ed. Engl.* **1993**, *32*, 1075.

Dendrimers: Self Assembly

Metal Complexation Mediated Self-Assembly

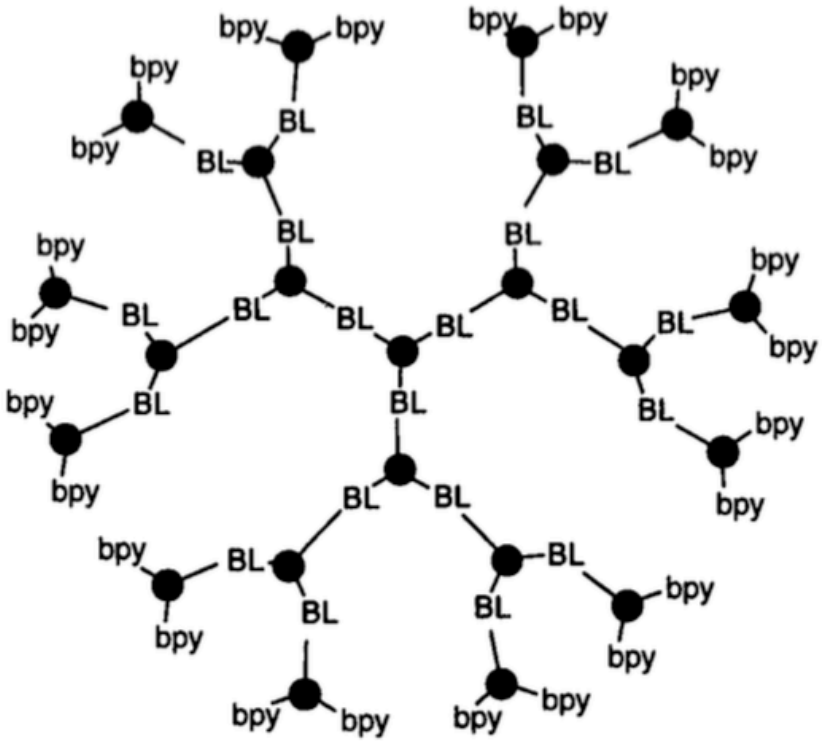

56

● = Ru^{2+}

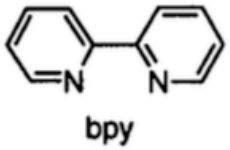

bpy

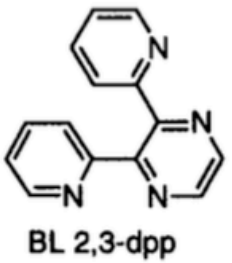

BL 2,3-dpp

57

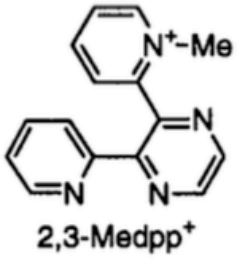

2,3-Medpp+

58

Balzani, *Gazz. Chim. Ital.* **1994**, *124*, 423

Dendrimers: Self Assembly

Metal Complexation Mediated Self-Assembly

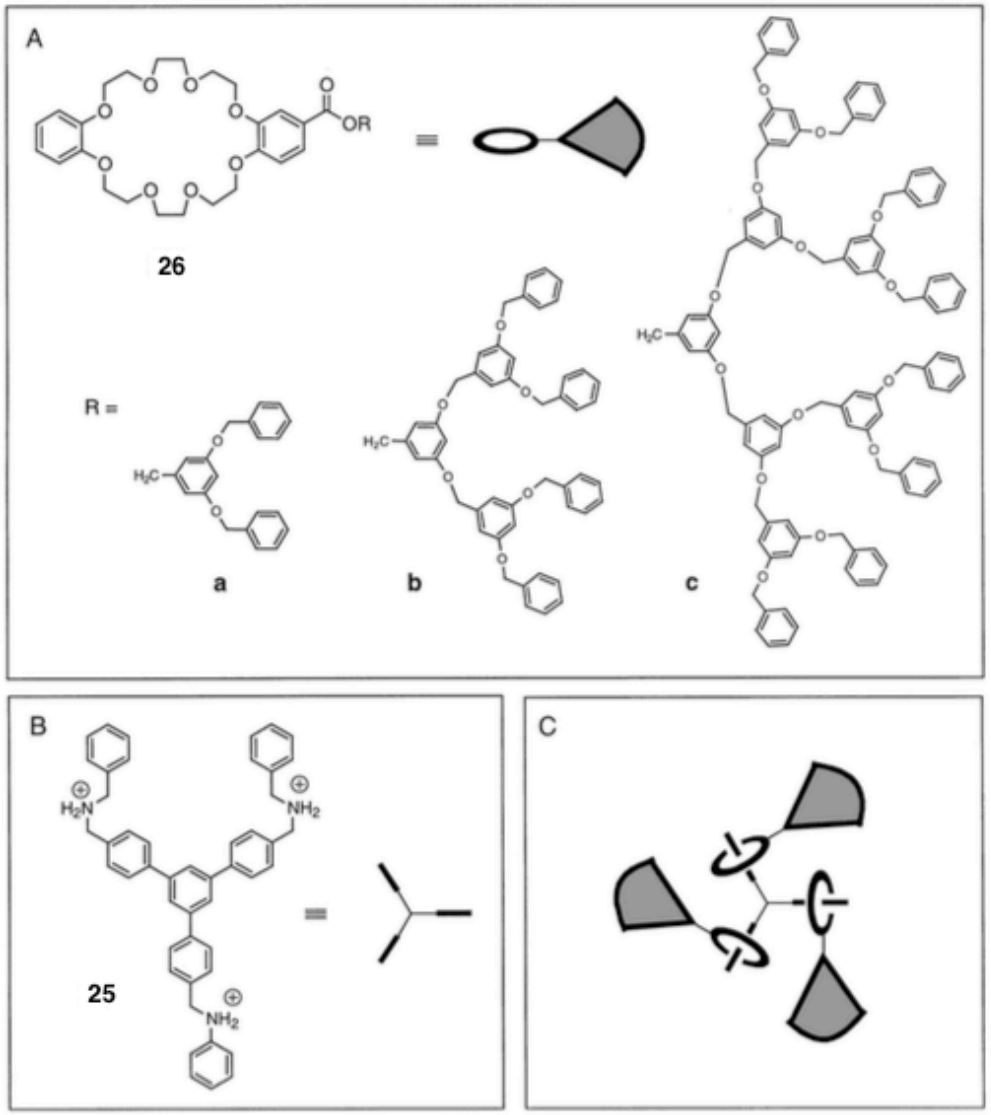

Fig. 8A–C. Gibson's self-assembling dendrimers using pseudorotaxanes formation: **A** crown-ethers with dendritic substituents; **B** triammonium ion core; **C** schematic of tridendron formed by triple pseudorotaxane self-assembly

Dendrimers: Self Organization

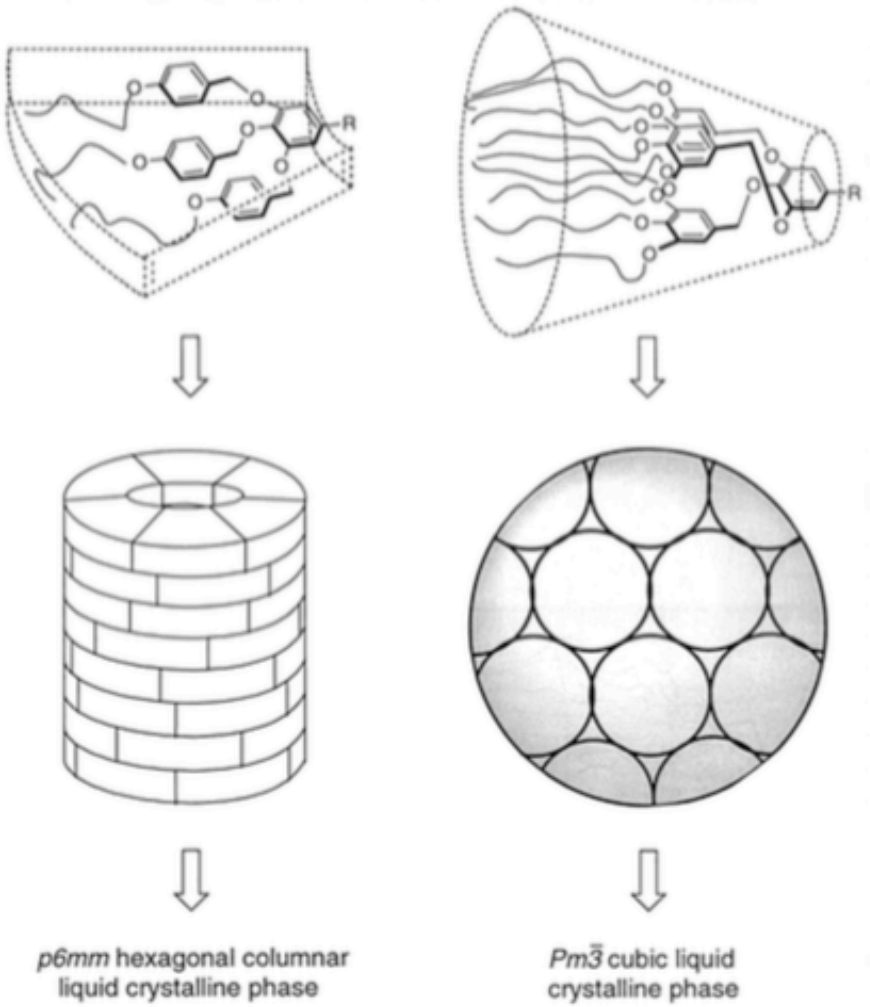

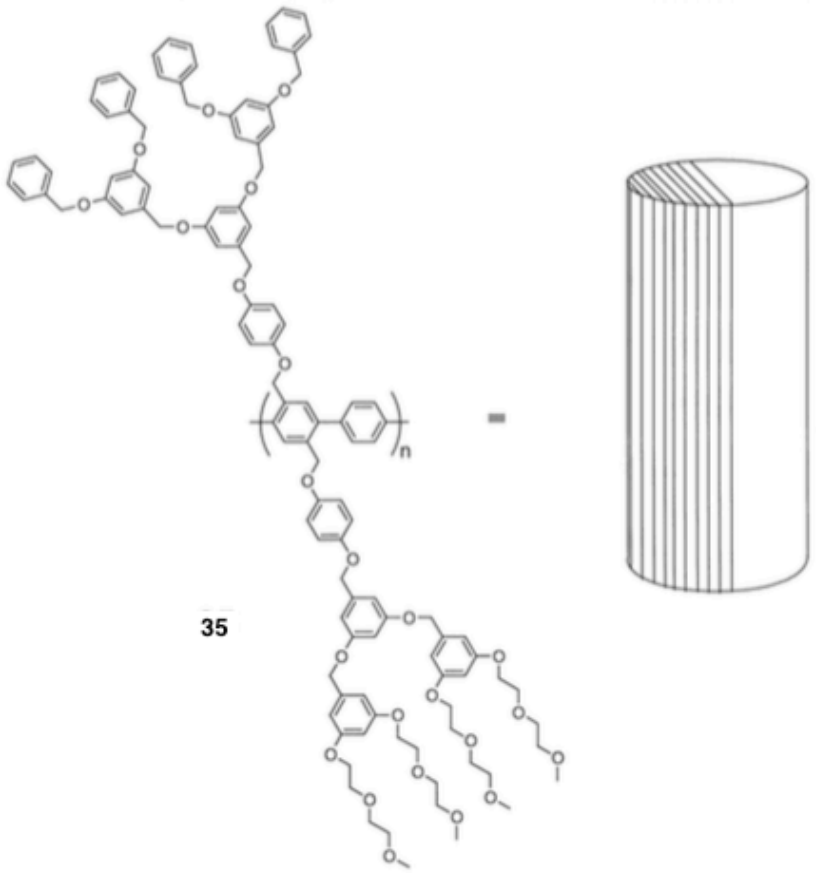

Fig. 14. Schlüter and coworkers synthesized dendritic rods (e.g., **35**) and reported the self-organization of amphiphilic structures with a dendritic PEG half (hydrophilic) and a Féchet-type dendritic segment (hydrophobic)

Percec

Chem Eur J **2000**, 6, 1258
Angew. Chem. Int. Ed. **2000**, *l39*,1598
J. Am. Chem. Soc. **2000**, *122*, 4249
J. Am. Chem. Soc. **2000**, 122, 1684
J Am Chem Soc **2000**, *122*, 10273

Dendrimers: Self Organization

Monolayers for the formation of nanorods

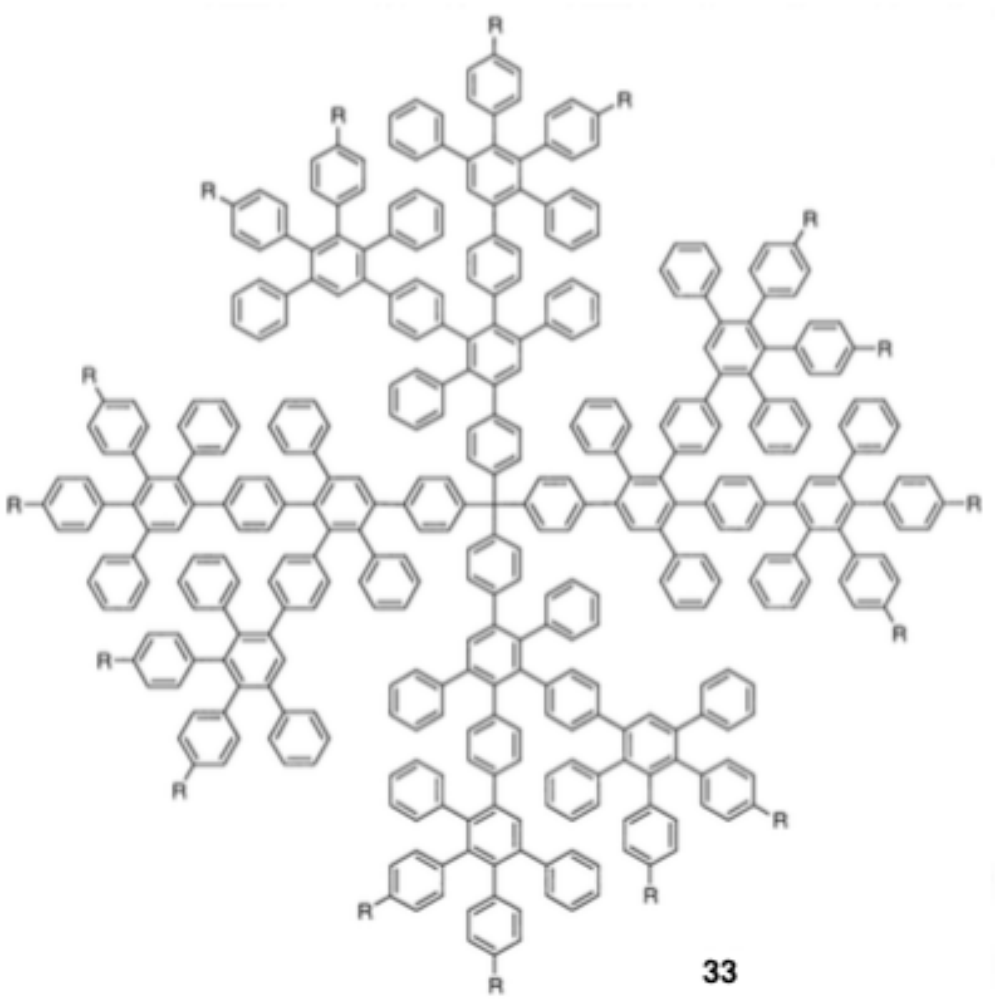

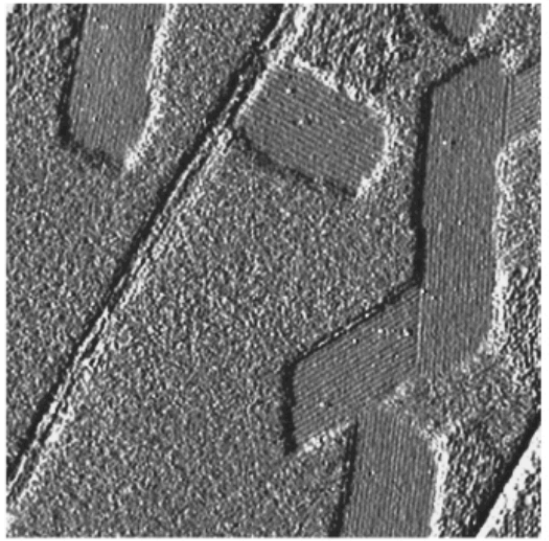

Fig. 2 AFM amplitude image (scan size 639 nm) of a dendrimer **1** layer on HOPG.

Müllen K, *Chem. Commun,* **2000**, 1169

Dendrimers: Self Organization

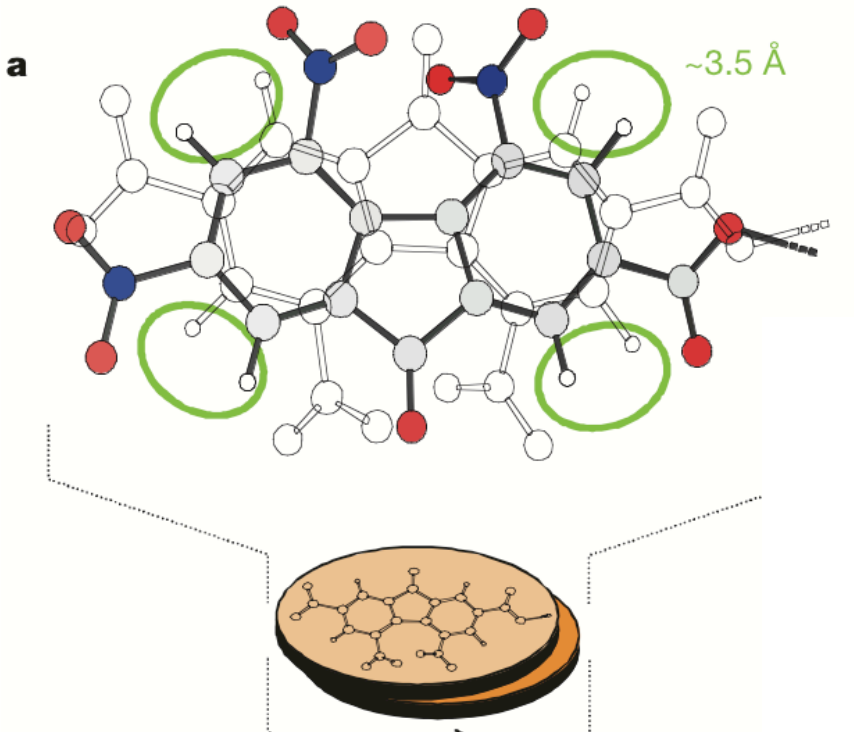

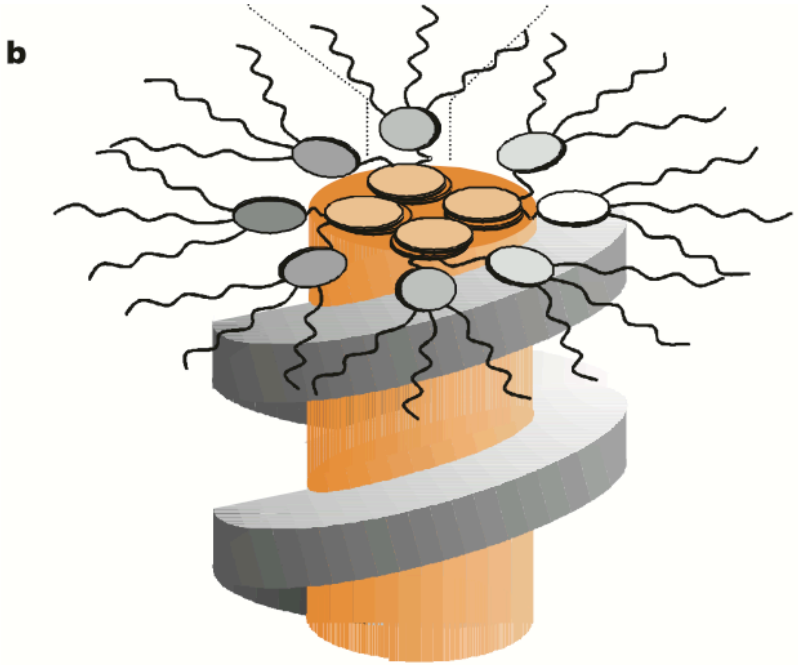

Percec, *Nature*, **2002**

Figure 5 The molecular arrangement in the supramolecular column self-assembled from **A1**. **a**, Sandwich-type stacking of the nitro-fluorenone moieties with proton–proton distances of 3.5 Å, as determined by ^{1}H-^{1}H double-quantum NMR spectroscopy. **b**, Structure of the supramolecular columns with stacks of fluorenone sandwiches in the centre of the columns, jacketed by helical dendrons.

Dendrimers: Host-Guest Chemistry

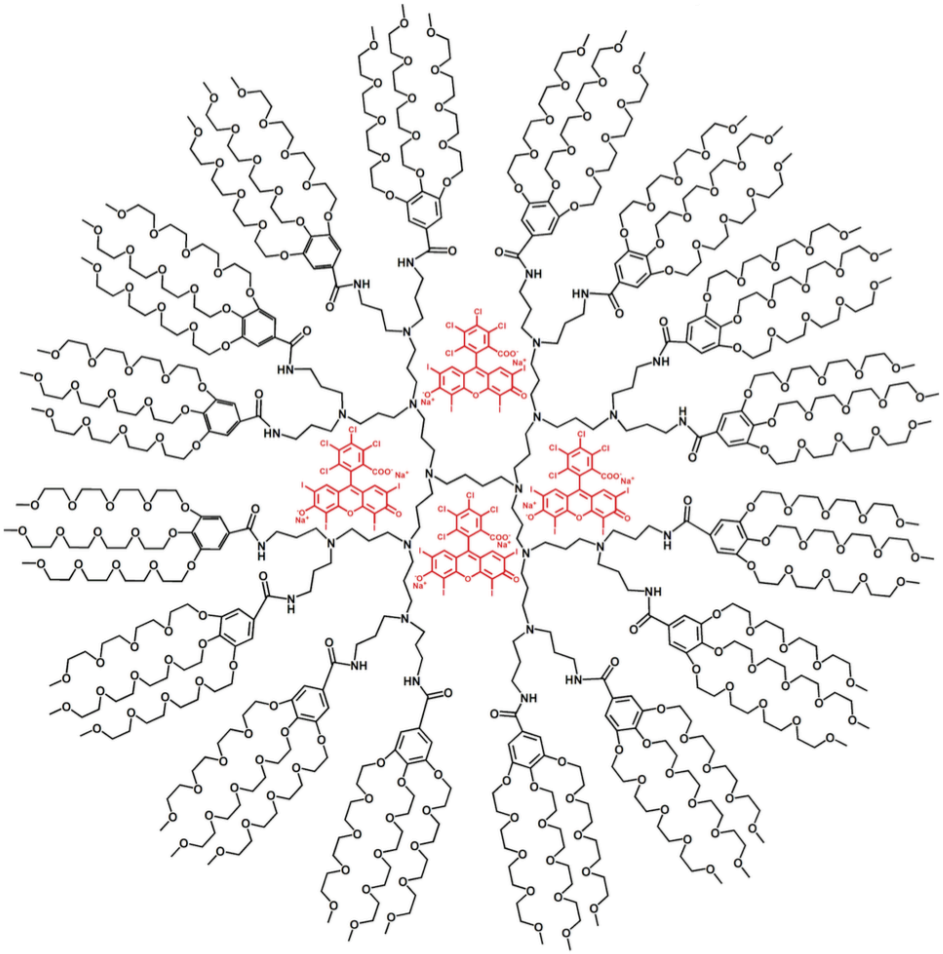

Oligoethyleneoxy-functionalized PPI Dendrimer with Rose Bengal

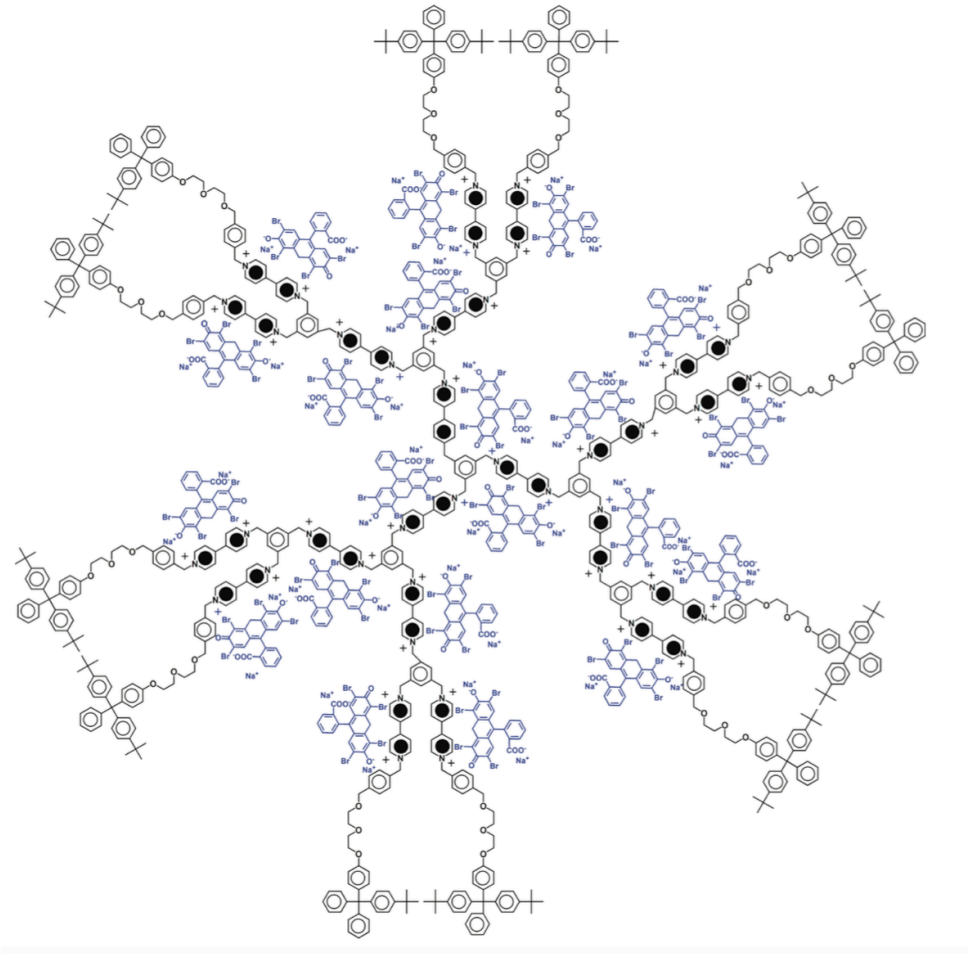

Dendrimer Containing Electron-Acceptor Viologen Units with Eosin

Cheng, *Chem. Rev.*, **2012**, 112, 3856

Dendrimers: Host-Guest Chemistry

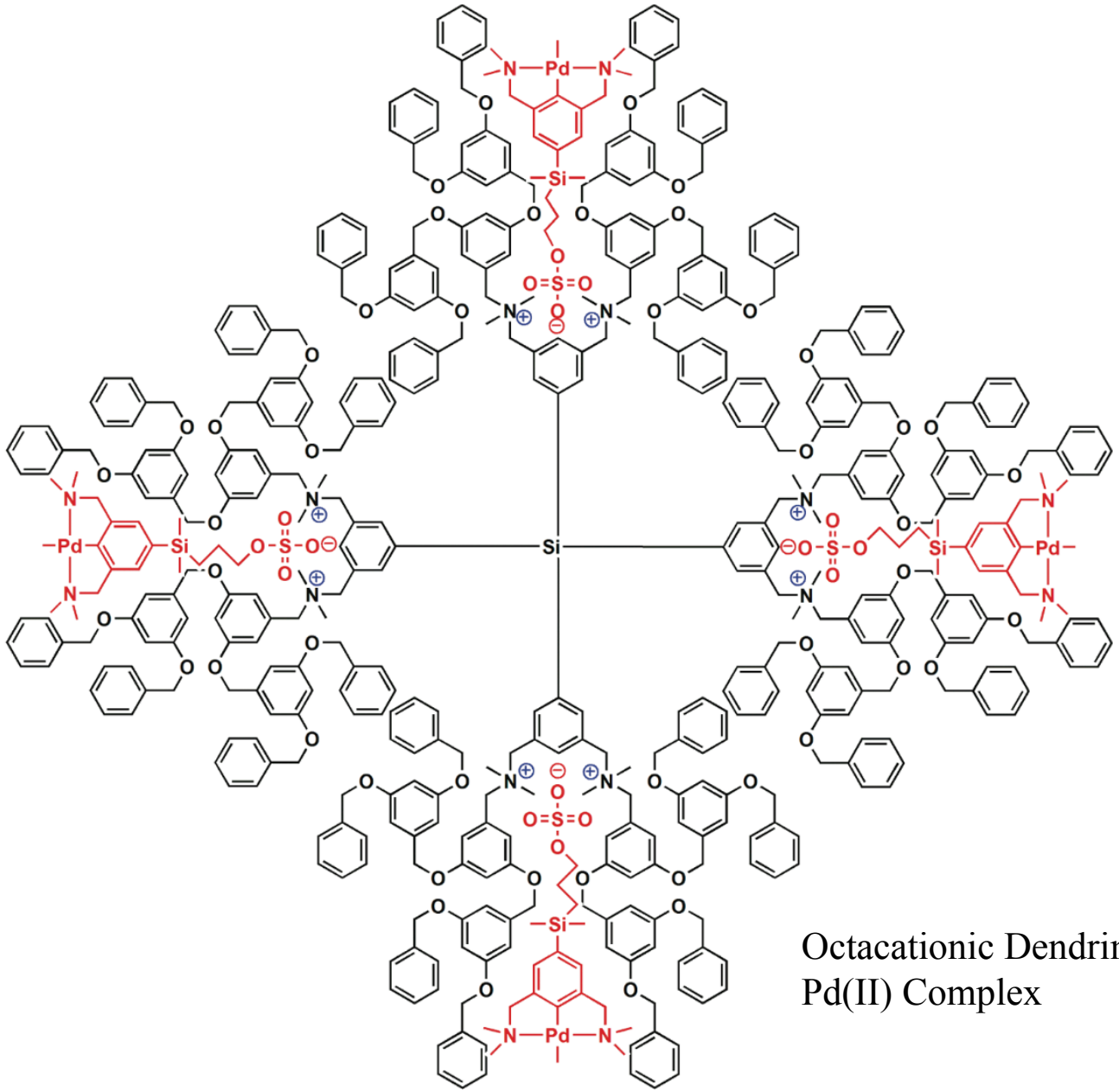

Octacationic Dendrimer with
Pd(II) Complex

Dendrimers and calixarenes

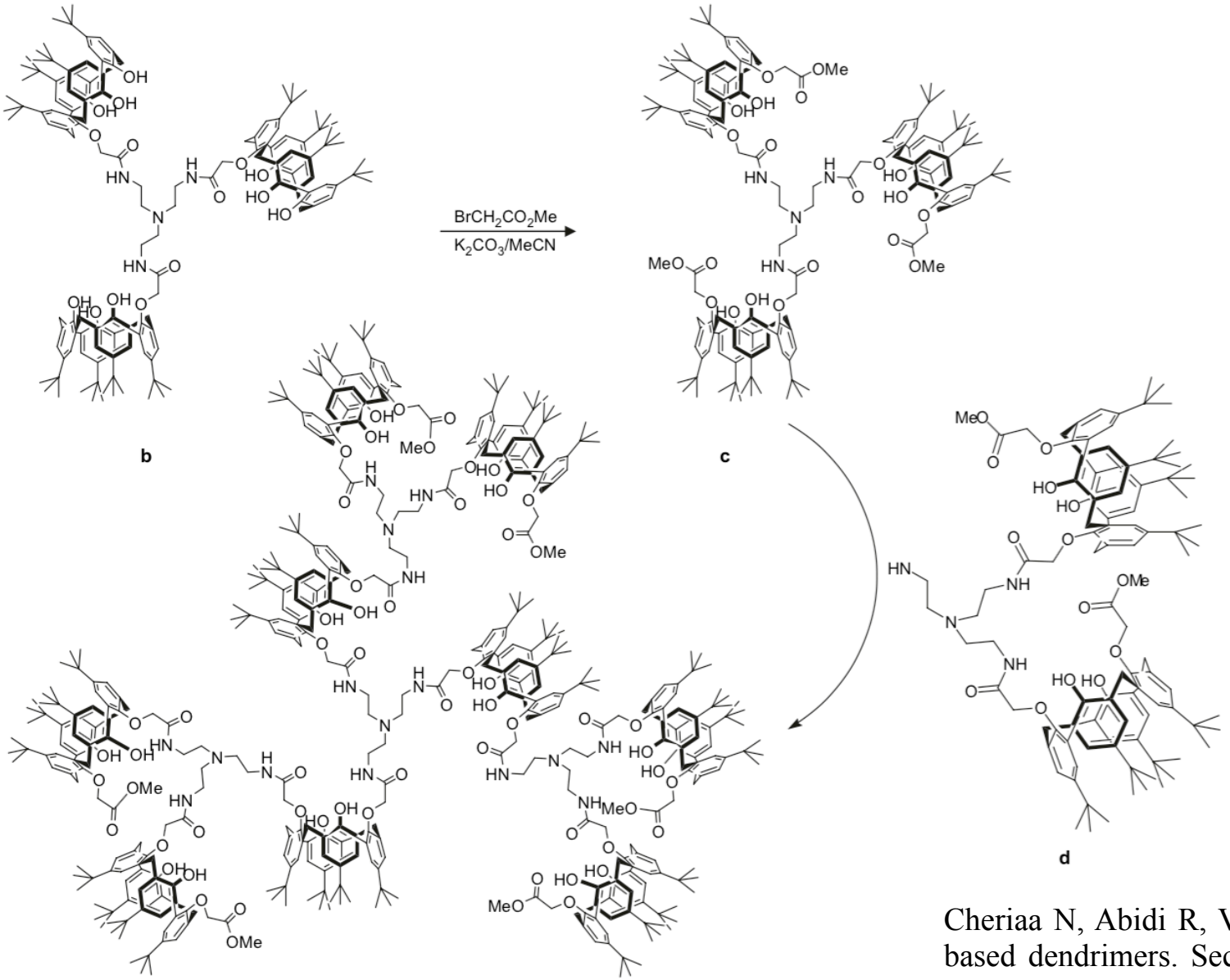

Scheme 35. Synthesis of a dendrimer possessing a calix[4]arene spacer [1376].

Cheriaa N, Abidi R, Vicens J. Calixarene-based dendrimers. Second generation of a calix[4]-dendrimer with a 'tren' as core. *Tetrahedron Lett* **2005**;46:1533e6.

Other examples:

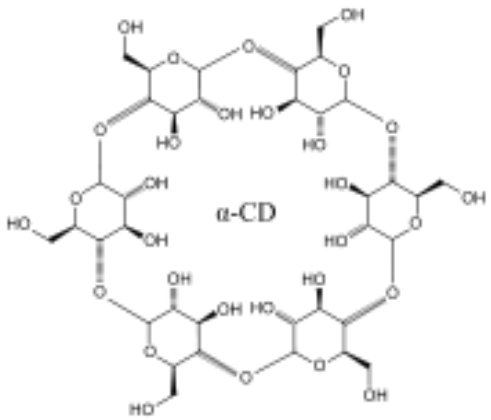

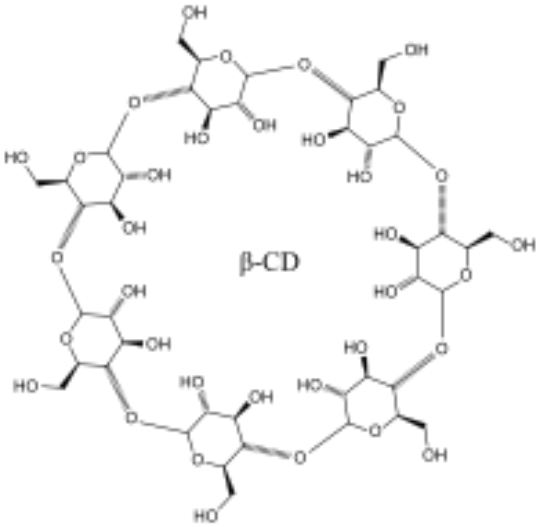

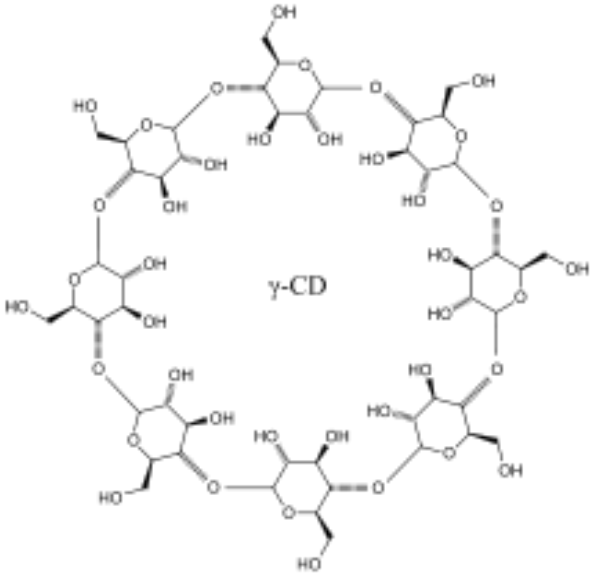

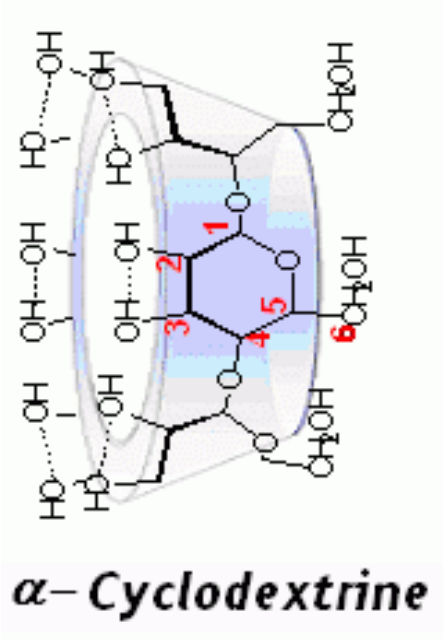

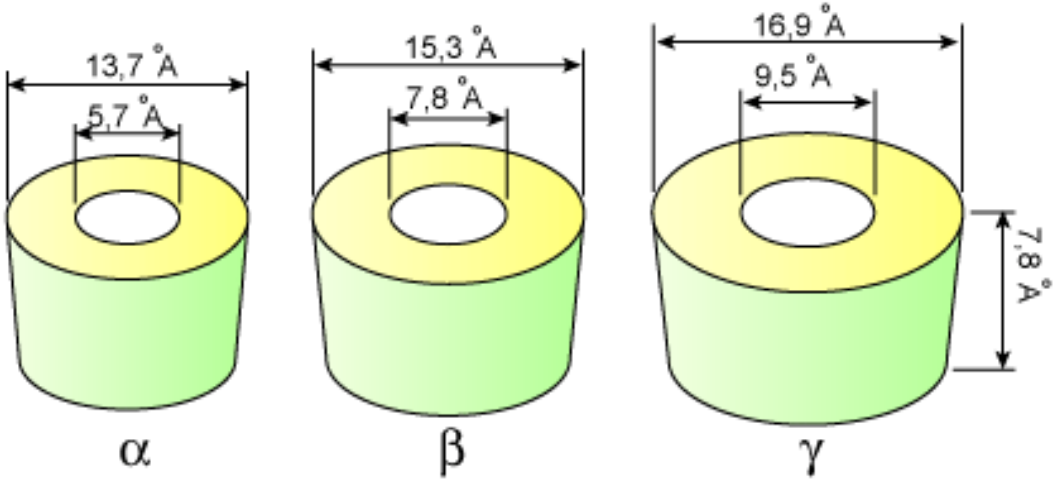

Cyclodextrines

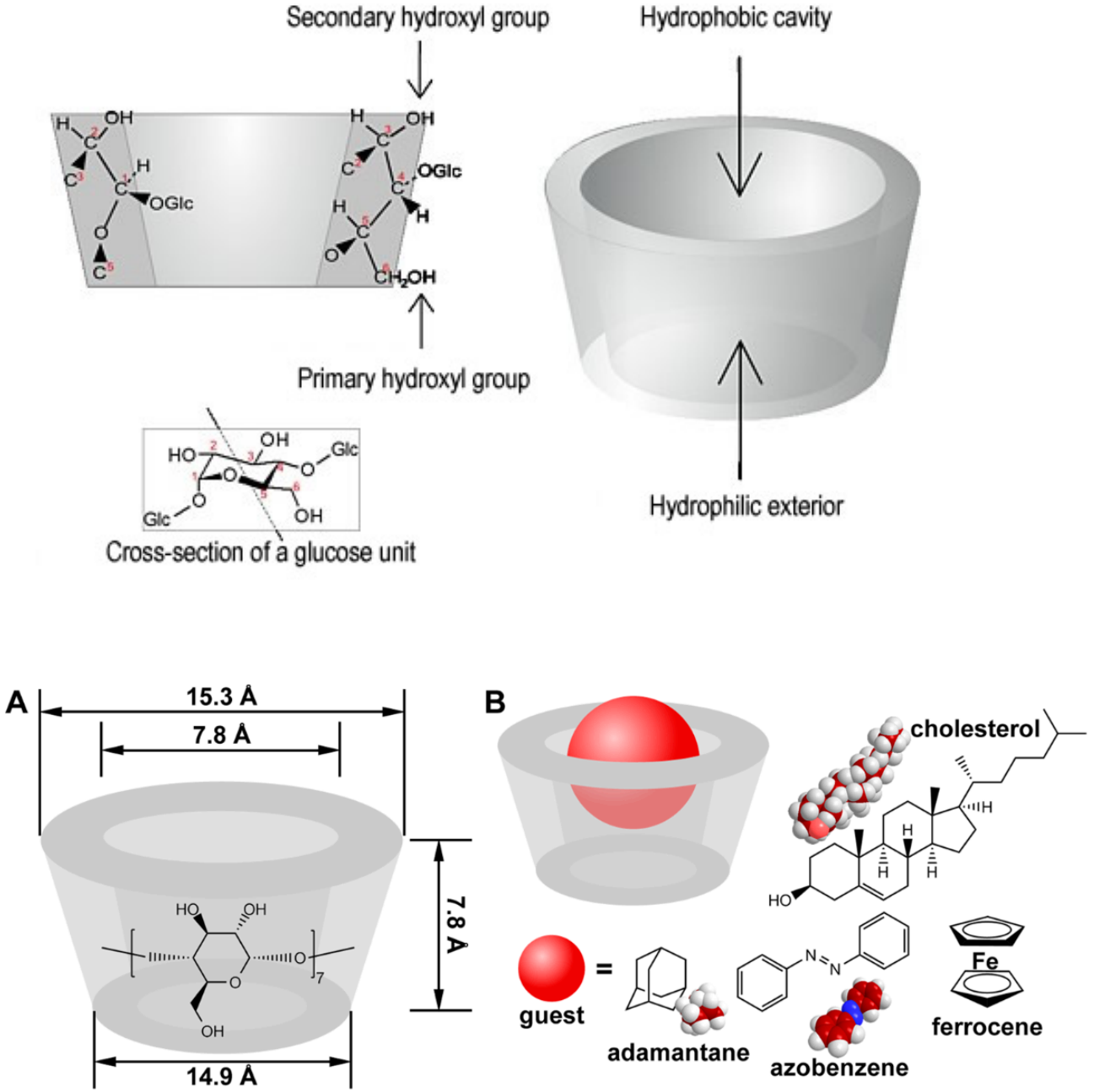

Figure 1. (A) Structure of βCD and (B) common guest molecules forming inclusion complexes with βCD host.

Cyclodextrines

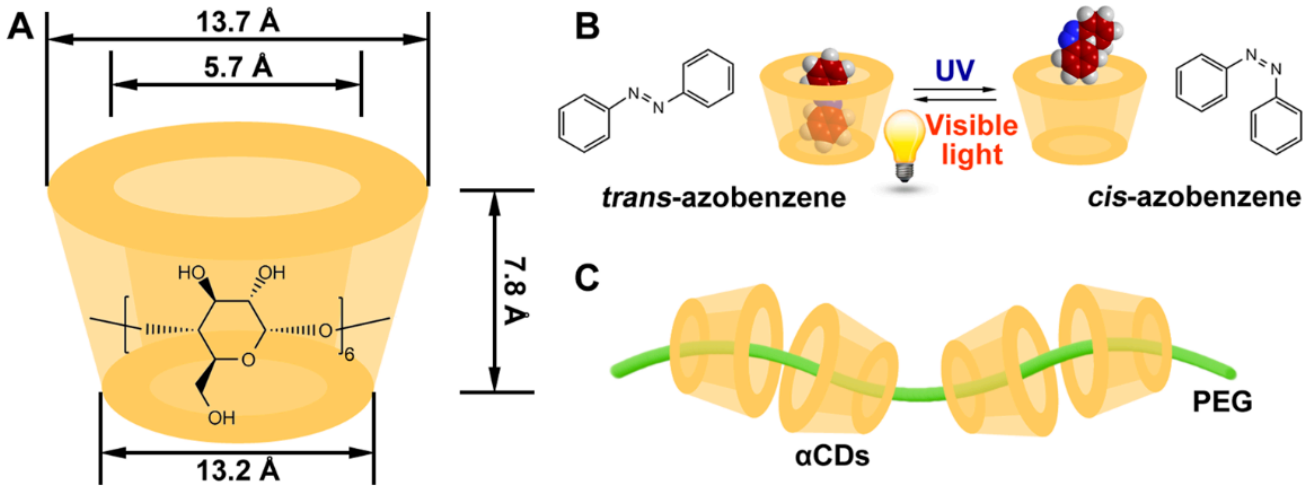

Figure 4. (A) Structure of αCD, (B) interaction of azobenzene and αCD enabling photoregulation based on azobenzene isomerization, and (C) αCDs threaded onto a PEG chain comprising the pseudopolyrotaxane architecture.

Chu et al., *Acc. Chem. Res.* **2014**, *47*, 2017

Cyclodextrines: self assembly and gold isolation

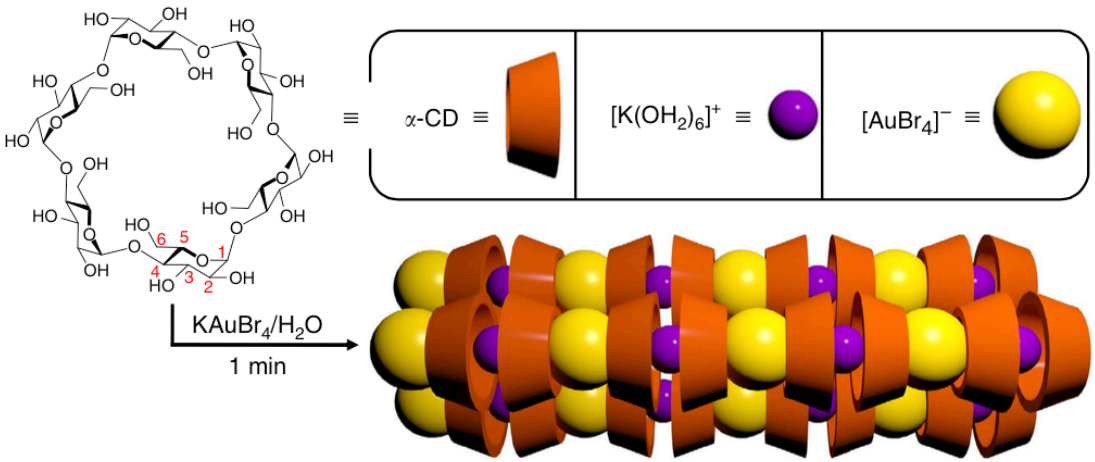

Figure 1 | Schematic representation of the spontaneous self-assembly of α•Br. Upon mixing $KAuBr_4$ and α-CD in water, a hydrogen-bonded linear superstructure forms spontaneously in <1 min. The cavities of the α-CDs oriented head-to-head, tail-to-tail form a continuous channel, which is filled by an alternating $[K(OH_2)_6]^+$ and $[AuBr_4]^-$ polyionic chain to generate a cable-like superstructure that then tightly packs one with another (Supplementary Fig. S1) leading to crystals observable to the naked eye.

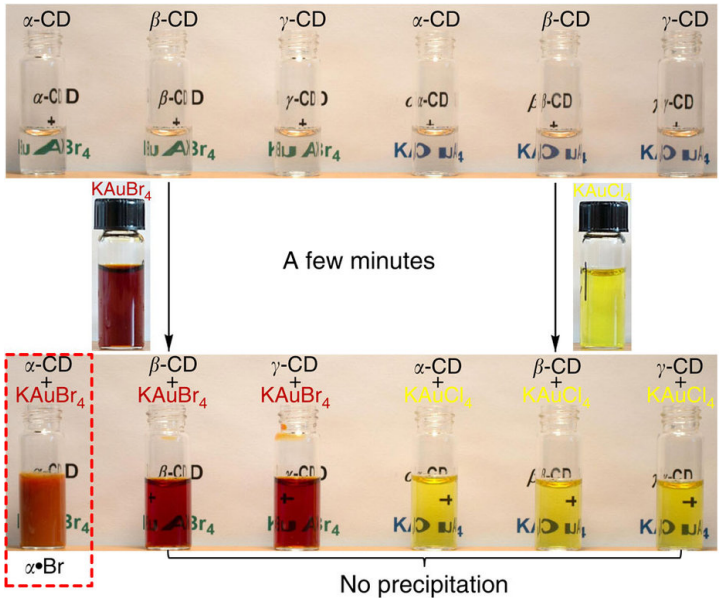

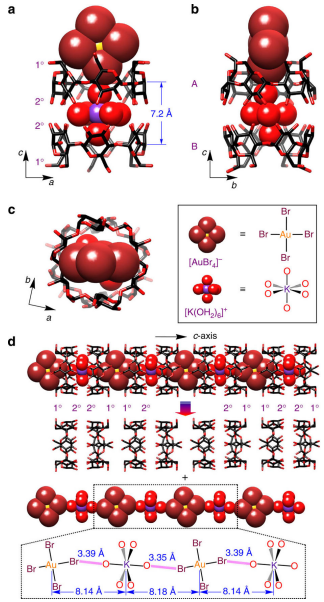

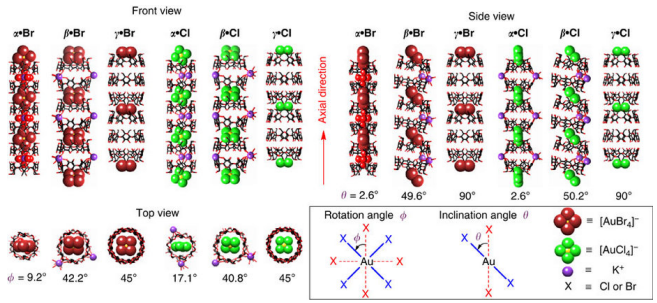

Fraser Stoddart, *Nature Commun.*, **2013**

Cyclodextrines: self assembly and gold isolation

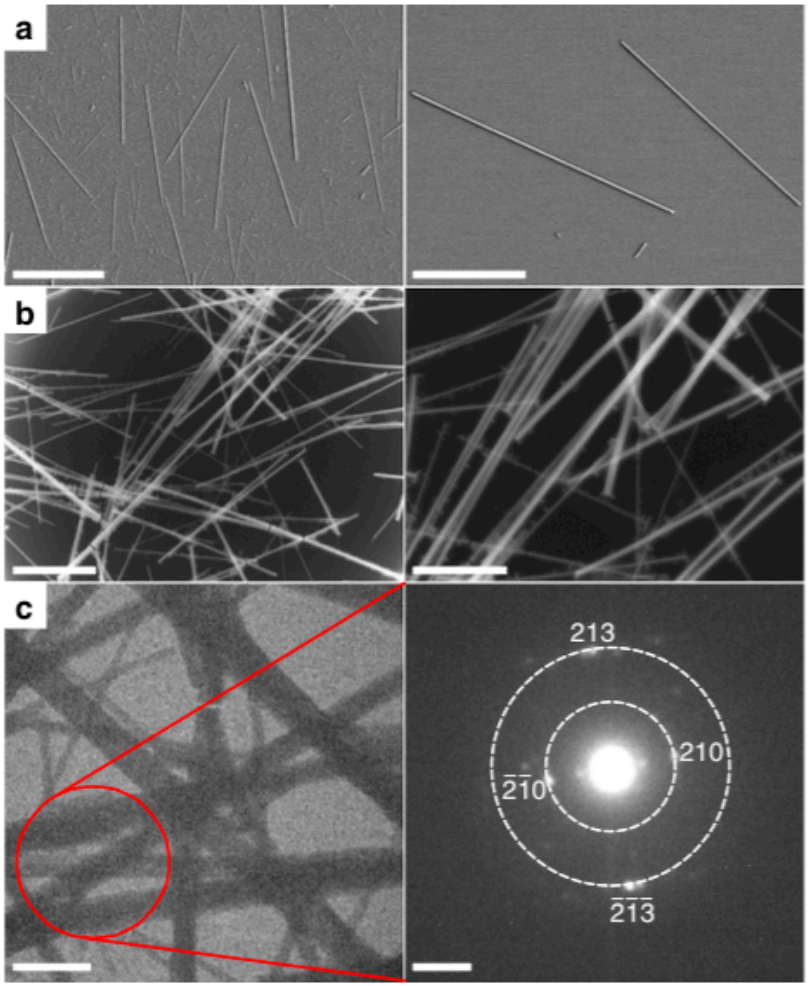

Fraser Stoddart, *Nature Commun.*, **2013**

Figure 3 | Morphology of the nanostructures of α•Br. (**a**) SEM images of a crystalline sample prepared by spin-coating an aqueous suspension of **α•Br** onto a silicon substrate, and then air-drying the suspension. (**b**) TEM images of **α•Br** prepared by drop-casting an aqueous suspension of **α•Br** onto a specimen grid covered with a thin carbon support film and air-dried. (**c**) Cryo-TEM image (left) and SAED pattern (right) of the nanostructures of **α•Br**. As the selected area includes several crystals with different orientations and the crystals are so small that the diffraction intensities are relatively weak, we can assign the diffraction rings composed of diffraction dots but not the specific angles between different diffraction dots from the same crystal. The scale bars in **a** and **b** are 25 (left), 5 (right), 10 (left), 5 μm (right) and in **c** are 1 μm (left) and 1 nm^{-1} (right), respectively.

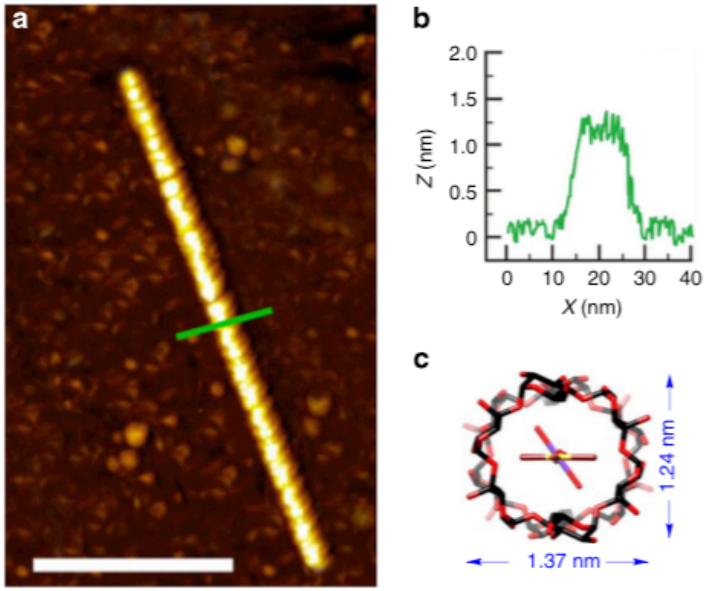

Figure 5 | AFM analysis of α•Br on a mica surface. (**a**) AFM image of a spin-coated sample of **α•Br** on a freshly cleaved mica surface. (**b**) The cross-sectional analysis of (**a**). (**c**) Dimensions of the cross-section of the one-dimensional α-CD channel in **α•Br**. Scale bar, 100 nm.

Host–Guest Systems

DOI: 10.1002/anie.200460675

The Cucurbit[*n*]uril Family

*Jason Lagona, Pritam Mukhopadhyay, Sriparna Chakrabarti, and Lyle Isaacs**

Keywords:
cucurbituril · molecular machines · molecular recognition · supramolecular chemistry

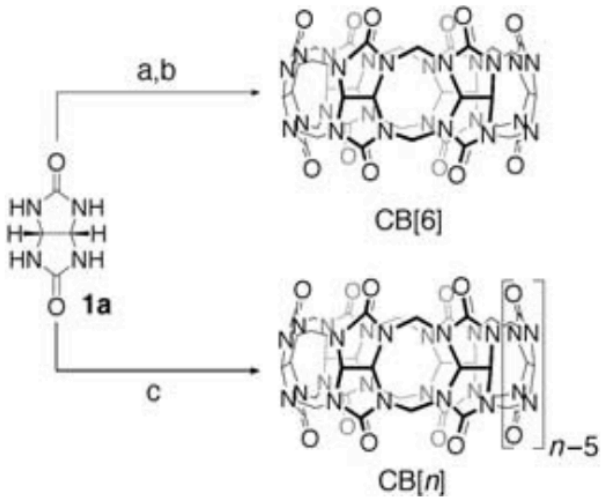

Scheme 1. Synthesis of CB[6] from **1a** under forcing conditions and a mixture of CB[n] under milder conditions. a) CH_2O, HCl, heat; b) H_2SO_4; c) CH_2O, HCl, 100 °C, 18 h.

Curcurbituril

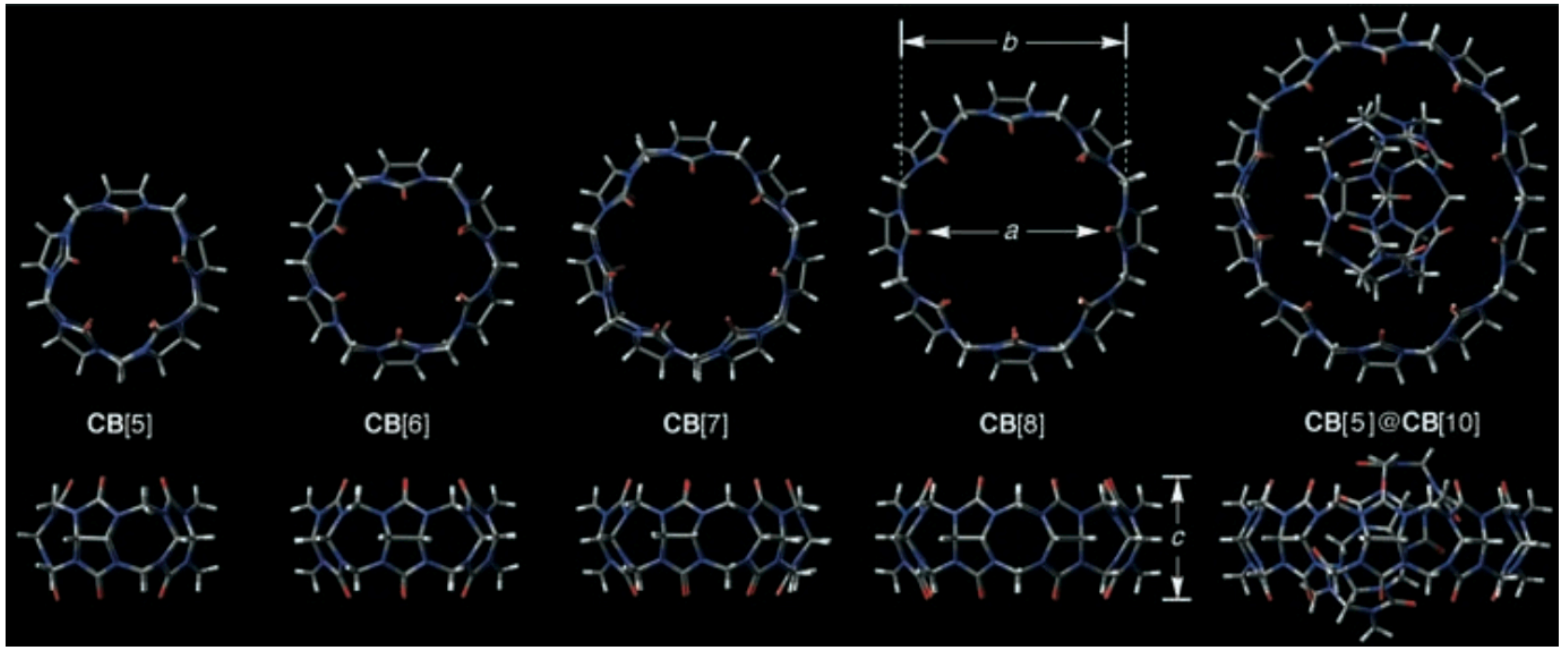

Figure 3. Top and side views of the X-ray crystal structures of CB[5],[7] CB[6],[2] CB[7],[7] CB[8],[7] and CB[5]@CB[10].[9] The various compounds are drawn to scale.

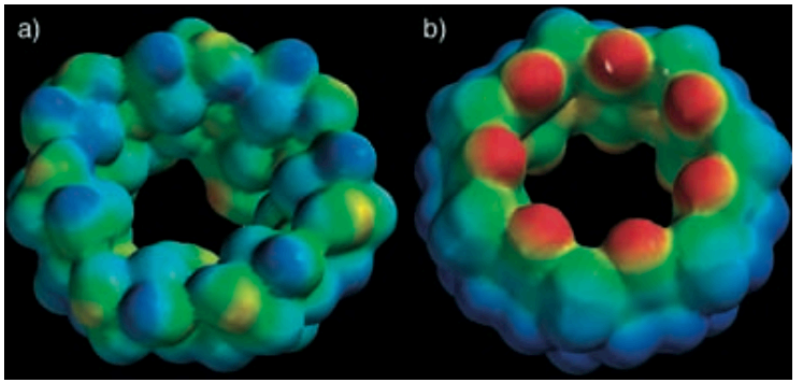

Figure 4. Electrostatic potential maps for a) β-CD and b) CB[7]. The red to blue color range spans −80 to 40 kcal mol^{-1}. Adapted from Kim and co-workers.[5]

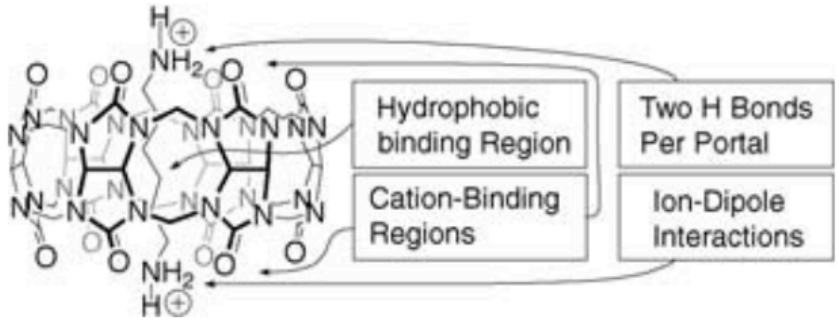

Figure 5. Representation of the different binding regions of CB[6] and the geometry of the complex between CB[6] and the hexanediammonium ion.

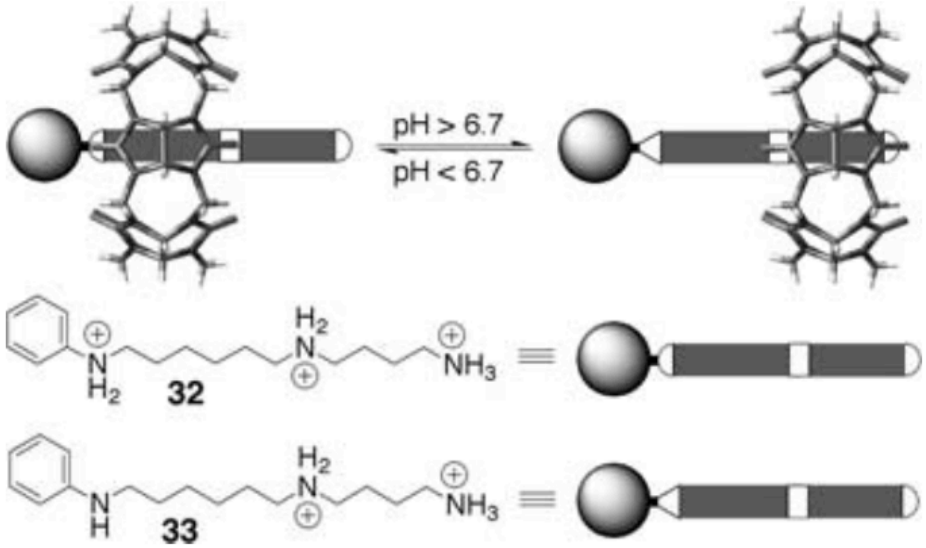

Scheme 5. CB[6]-based molecular switch.

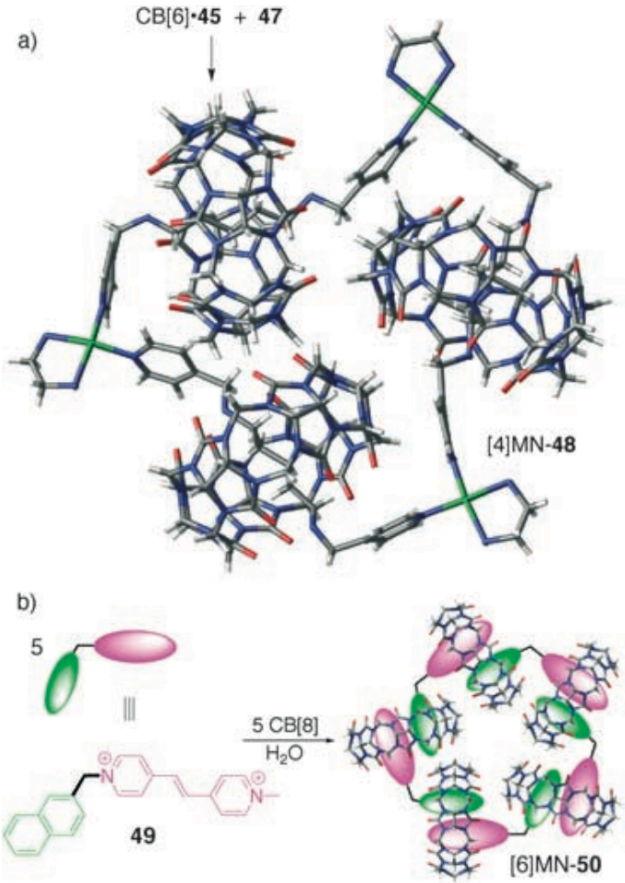

Scheme 11. Formation of molecular necklaces using: a) CB[6] and b) CB[8] as beads.

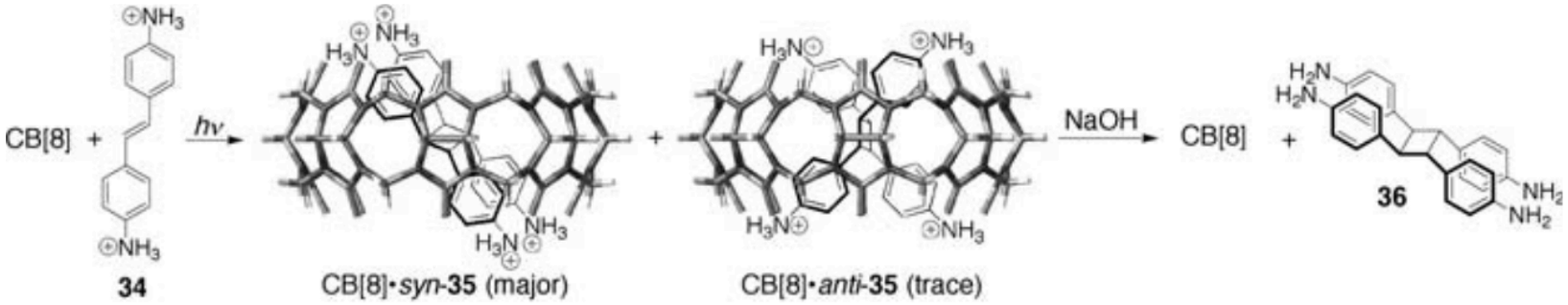

Scheme 6. [2+2] photoaddition reaction mediated by CB[8].

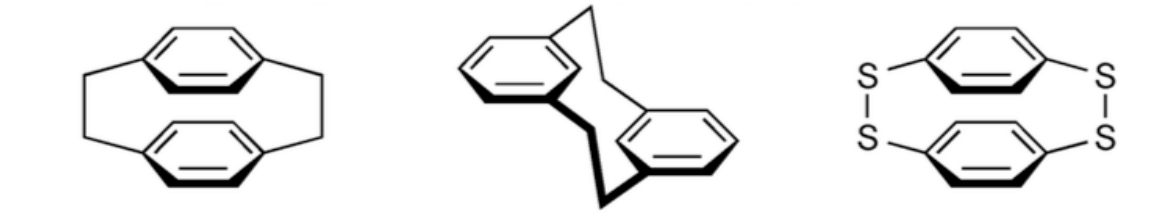

1
Brown and Farthing, 1949
Cram 1951

2
Pellegrin, 1899

3
Parekh and Guha, 1934

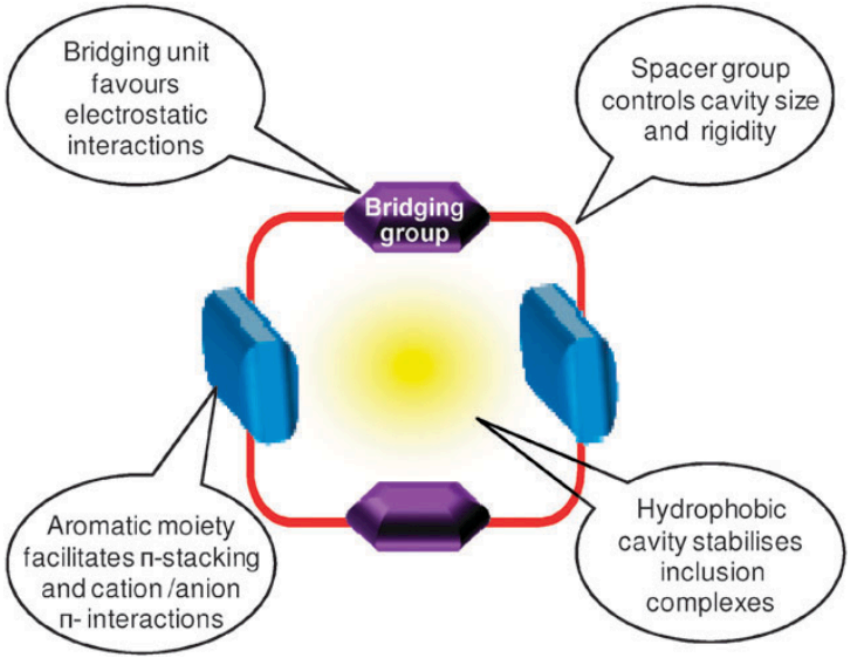

Fig. 1 Schematic representation of binding sites in a functionalised cyclophane system.

Cyclophanes: molecular recognition

D. Ramaiah, *Org. Lett.*, **2005**, *7*, 5765

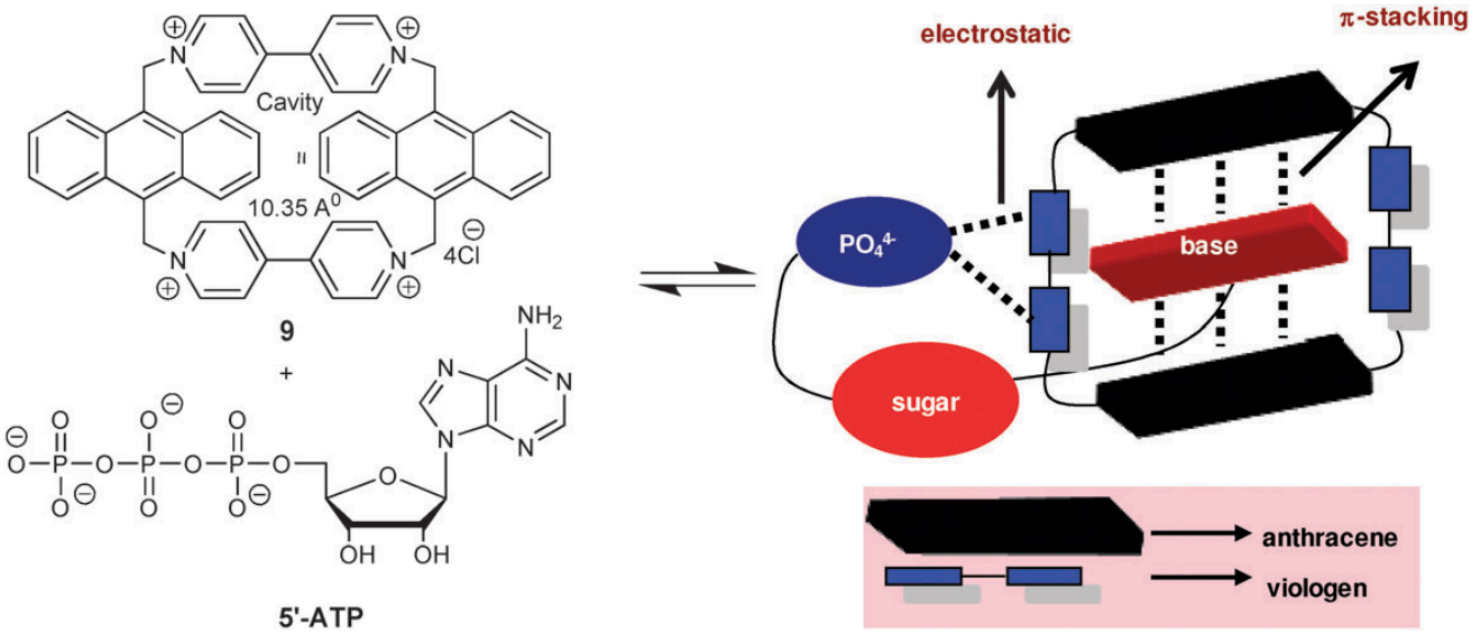

Fig. 10 Schematic representation of recognition of 5′-ATP by cyclophane **9**. Reprinted with permission from ref. 41. Copyright 2009 American Chemical Society.

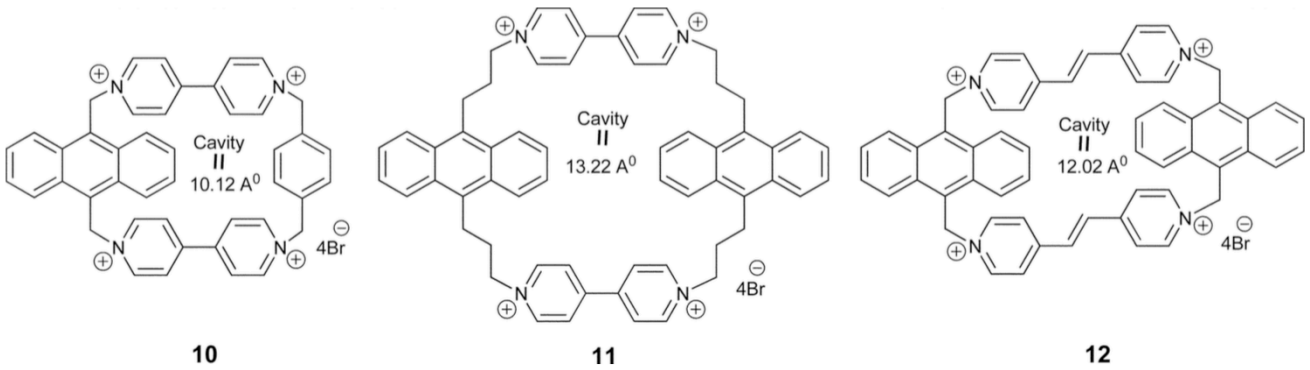

Fig. 12 Structure of cyclophanes **10–12**.